

Accepted Manuscript

Synthesis, cytotoxic activity, and tubulin polymerization inhibitory activity of new pyrrol-2(3*H*)-ones and pyridazin-3(2*H*)-ones

Samar Hafez Abbas, Gamal El-Din A.A. Abuo-Rahma, Mohamed Abdel-Aziz, Omar M. Aly, Eman A. Beshr, Amira M. Gamal-Eldeen

PII: S0045-2068(16)30026-8

DOI: <http://dx.doi.org/10.1016/j.bioorg.2016.03.007>

Reference: YBIOO 1894

To appear in: *Bioorganic Chemistry*

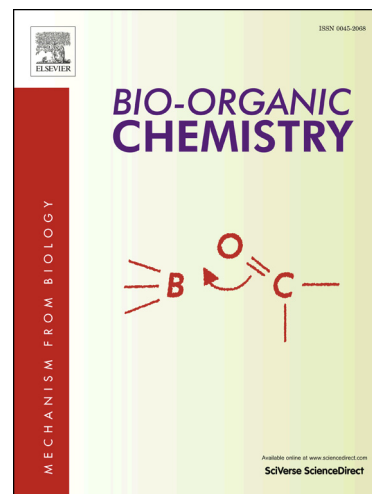
Received Date: 8 October 2015

Revised Date: 13 March 2016

Accepted Date: 14 March 2016

Please cite this article as: S.H. Abbas, G.E-D. Abuo-Rahma, M. Abdel-Aziz, O.M. Aly, E.A. Beshr, A.M. Gamal-Eldeen, Synthesis, cytotoxic activity, and tubulin polymerization inhibitory activity of new pyrrol-2(3*H*)-ones and pyridazin-3(2*H*)-ones, *Bioorganic Chemistry* (2016), doi: <http://dx.doi.org/10.1016/j.bioorg.2016.03.007>

This is a PDF file of an unedited manuscript that has been accepted for publication. As a service to our customers we are providing this early version of the manuscript. The manuscript will undergo copyediting, typesetting, and review of the resulting proof before it is published in its final form. Please note that during the production process errors may be discovered which could affect the content, and all legal disclaimers that apply to the journal pertain.



Synthesis, cytotoxic activity, and tubulin polymerization inhibitory activity of new pyrrol-2(3*H*)-ones and pyridazin-3(2*H*)-ones

Samar Hafez Abbas^a, Gamal El-Din A. A. Abuo-Rahma^{a*}, Mohamed Abdel-Aziz^a, Omar M. Aly^a, Eman A. Beshr^{a,b}, Amira M. Gamal-Eldeen^c

^a Medicinal Chemistry Department, Faculty of Pharmacy, Minia University, Minia, 61519, Egypt.

^{a,b} Department of Pharmaceutical Chemistry, College of Pharmacy, Umm Al-Qura University, Makkah 21955, Saudi Arabia.

^c Cancer Biology Laboratory, Center of Excellence for Advanced Sciences, National Research Center, Dokki, Giza, Egypt.

*Corresponding author. Tel.: +201003069431. Fax.: +2086-2369075

E-mail address: gamal.aborahma@mu.edu.eg

Postal address: Medicinal Chemistry Department, Faculty of Pharmacy, Minia University, Minia, 61519, Egypt.

Abstract

A series of new pyrrol-2(3*H*)-ones **4a-f** and pyridazin-3(2*H*)-ones **7a-f** were synthesized and characterized using different spectroscopic tools. Some of the tested compounds revealed moderate activity against 60 cell lines. The *E* form of the pyrrolones **4** showed good cytotoxic activity than both the *Z* form and the corresponding open amide form. Furthermore, the *in vitro* cytotoxic activity against HepG2 and MCF-7 cell lines revealed that compounds (*E*)**4b**, **6f** and **7f** showed good cytotoxic activity against HepG2 with IC₅₀ values of 11.47, 7.11 and 14.80 μM, respectively. Compounds (*E*)**4b**, **6f**, **7d** and **7f** showed a pronounced inhibitory effect against cellular localization of tubulin. Flow cytometric analysis indicated that HepG2 cells treated with (*E*)**4b** showed a predominated growth arrest at the S-phase compared to that of G2/M-phase. Molecular modeling study using MOE[®] program indicated that most of the target compounds showed good binding of β-subunit of tubulin with the binding free energy (dG) values about -10 Kcal/mole.

Keywords: Pyrrolone; pyridazinone; Cytotoxicity; Tubulin; immunofluorescence, docking study.

1. Introduction

Tubulin is a globular protein that represents an important target for anticancer drug discovery. A variety of natural compounds including podophyllotoxin, colchicine, steiganacine and combretastatins (CAs) inhibit tubulin polymerization by binding to

colchicine binding site. In fact, CAs causes a pronounced shutdown in blood flow to solid tumors, resulting in extensive tumor-cell necrosis. Among CAs products, combretastatin A4 (**I**) which represents one of the most potent antitumor agents; it shows strong cytotoxicity against a variety of cell lines and is considered one of the powerful vascular disrupting agents.¹

The structural feature of the CAs include: a *cis* double bond, a trimethoxy- phenyl ring "A" and a small substituent on the ring B. Conversion of *cis* double bond into *trans* one produces dramatic reduction in both antitubulin and cytotoxicity. Substitution of the olefinic bond by a heterocyclic ring gave compounds with potent antimitotic properties such as compounds **II**², **III**³, **IV**⁴ and **V**⁵ (**Fig. 1**). This suggestion supports the fact that; modification of the double bond could produce effective antimitotic agents. The structural modifications to ring A had received very little attention. Most CAs derivatives retained the trimethoxyphenyl moiety. Keira's research group showed no necessity of the three methoxy groups in ring A for optimum biological activity such as compound **VI** (**Fig. 1**).⁶

The potent cytotoxicity and structural simplicity of combretastatin, has been envisaged as a very attractive lead. In fact, the *cis* configured C–C double bond of CA-4 is prone to isomerize to the *trans*-form during storage and administration thus producing dramatic reduction in both antitubulin activity and cytotoxicity. Therefore, considerable efforts have gone into modifying combretastatin and discovering its bioavailable *cis*-restricted analogues based on the bioisosteric replacement of olefinic double bond of the natural product with vicinal diaryl-substituted five membered heteroaromatic rings including oxazole, isoxazole, thiazole, pyrazole, tetrazole and imidazole.⁴

Furanone ring system has interesting attraction because of the flexibility of its conversion into several heterocyclic systems of biological importance such as pyrrolone, pyridazine, oxadiazole and triazole derivatives.⁷ Moreover, furanone is widely recognized as a component of natural products that possess a wide range of interesting biological activities such as anti-inflammatory, anticancer. Also, different classes of synthetic furanones and pyrrolones possess a wide spectrum of important pharmacological activities such as antibacterial,^{8, 9} antifungal,¹⁰ anticancer,^{11, 12} anti-inflammatory,^{13, 14} vasodilation¹⁵ and anticonvulsant.¹³ Also, pyridazinones represent an important class of heterocyclic compounds, which have been extensive research due to their broad biological activities, such as anti-inflammatory¹⁶, analgesic,¹⁷ antihypertensive,¹⁸ anticancer,¹⁹ anti-diabetic²⁰, anticonvulsant,²¹ antimicrobial²² and antifungal activities²³.

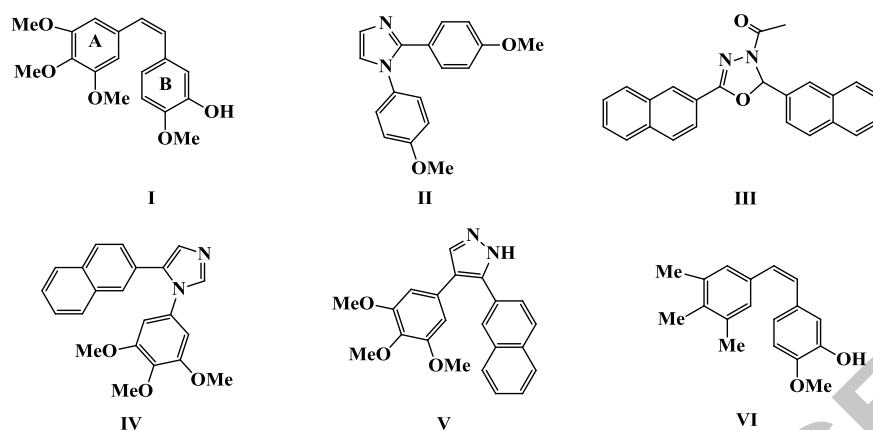


Fig. 1. Chemical structure of CA-4 (I) and its analogues II-VI.

Promoted with the above mentioned promising aspects, and in order to further investigate structural determinants of cytotoxic activity of this class of compounds, the present study involves a flexible, concise, and highly convergent protocol for the synthesis of pyrrolone and pyridazinone derivatives aiming at preparation of new combretastatin analogues with restricted rotation of both ring A and ring B. The prepared compounds were evaluated for both in vitro cytotoxic activity against liver carcinoma Hep-G2 and breast carcinoma MCF-7 cell lines. Moreover, tubulin polymerization inhibitory activity expressed in the localization of tubulin was explored in Hep-G2 cell line after treated with selected promising compounds as indicated by ELISA through immunofluorescence labeling and analysis under Apo time fluorescence microscope. Also, to explore the alteration in the cell cycle phases after treatment with the active cytotoxic compounds (*E*) **4b**, the cells were subjected to flow cytometry analysis. In addition, Docking of the target compound was done using MOE Program and X-ray crystallographic structure of tubulin complexes with colchicines.

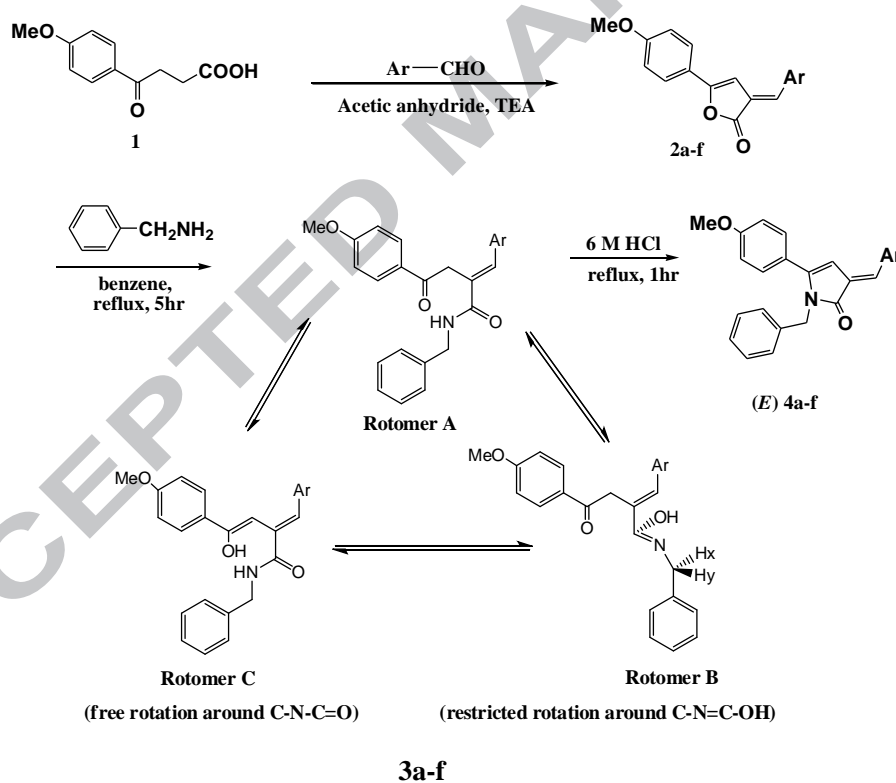
2. Results and Discussion

2.1. Chemistry

3-Arylidene-5-(4-methoxyphenyl)-2-(3*H*)-furanones **2a-f** were synthesized by fusion of the acid **1** and different appropriate aromatic aldehyde in the presence of TEA in acetic anhydride (Scheme 1) according to modified Perkin reaction.¹⁴ The chemical structure of furanones **2a-f** was elucidated on the basis of their IR, ¹H-NMR, mass spectra as well as the elemental analyses. Calculation of the δ values of furanones **2a-f** analogues using

incremental parameters for the hydrogen (semicyclic double bond) suggested the (*E*) configuration as reported in the literature.⁸⁻¹⁰

Heating at reflux of furanones **2a-f** with benzylamine in equimolar ratio in dry benzene afforded the corresponding amide derivatives¹⁵ **3a-f**. The chemical structures of the amides **3a-f** were elucidated on the basis of their IR, ¹H-NMR, mass spectrum as well as the elemental analysis. In the ¹H-NMR of amides **3**, it is noteworthy noting that the two benzylic –CH₂– protons are diastereotopic and appeared as two doublets. This may be attributed to the expected tautomerism in these compounds (Scheme 1). Heating at reflux of amides **3a-f** with 6 M hydrochloric acid for 1 h afforded the corresponding pyrrolones **4a-f** as reported in the literature.¹⁴ The chemical structure of the pyrrolones **4a-f** was confirmed by IR, ¹H-NMR, ¹³C-NMR, mass spectra as well as elemental analyses. X-ray crystallography of compound **4d** (Figure 2) revealed that the proper configuration of this compound is the kinetically stable (*E*) configuration.



2a, 3a, 4a; Ar = C₆H₅, **2b, 3b, 4b;** Ar = 4-OCH₃-C₆H₄, **2c, 3c, 4c;** Ar = 3,4,5-tri-OCH₃-C₆H₂, **2d, 3d, 4d;** Ar = 2-OH-C₆H₄, **2e, 3e, 4e;** Ar = 4-OH-3-OCH₃-C₆H₃ and **2f, 3f, 4f;** Ar = 4-Cl-C₆H₄.

Scheme 1. Synthesis of furanone derivatives **2a-f**, amide derivatives **3a-f** and (*E*) pyrrolone derivatives **4a-f**.

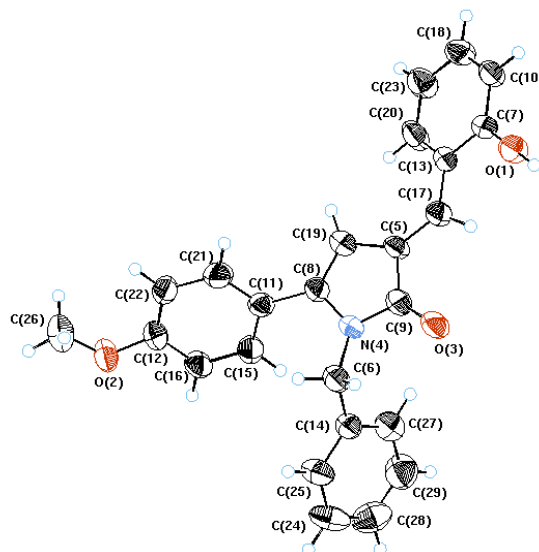
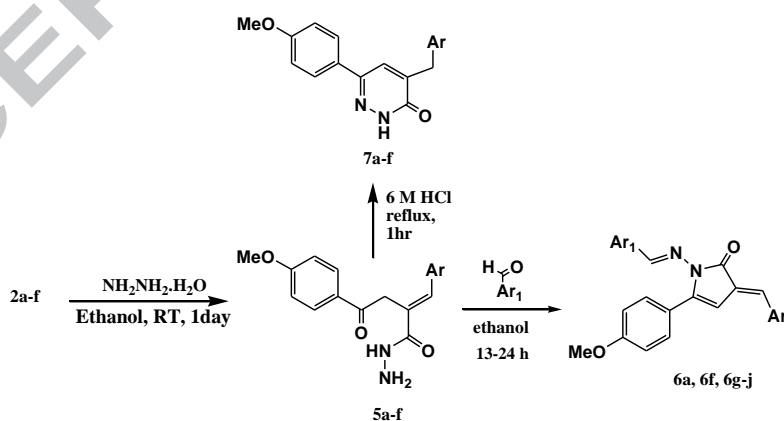


Fig. 2. The crystal structure of pyrrolone (*E*) **4d**.

It is noteworthy noting that, the *E* configuration of **3a-f** favors on *Z* configuration because of ring closure of the amides **3a-f** in (*Z*) configuration, don't occurred due to long distance between oxygen and amide nitrogen.

Reaction of furanone derivatives **2a-f** with hydrazine monohydrate afforded the corresponding hydrazide **5a-f**. Heating at reflux of *p*-methoxybenzaldehyde and hydrazides **5a** or **5f** for 13-24 h in ethanol afforded the corresponding pyrrolones **6a** & **6f**. Also, the pyrrolones **6g-j** was prepared by stirring of hydrazide **5f** with aromatic aldehyde in ethanol at room temperature for 2 days. (Scheme 2). The chemical structure of the pyrrolones **6a**, **6f** and **6g-j** was confirmed by IR, ¹H-NMR, mass spectra as well as elemental analysis.



5a, 7a; Ar = C₆H₅, **5b, 7b;** Ar = 4-OCH₃-C₆H₄, **5c, 7c;** Ar = 3,4,5-tri-OCH₃-C₆H₂,
5d, 7d; Ar = 2-OH-C₆H₄, **5e, 7e;** Ar = 4-OH-3-OCH₃-C₆H₃, **5f, 7f;** Ar = 4-Cl-C₆H₄.
In 6; **6a:** Ar = Ar₁ = 4-OCH₃-C₆H₄, **6f:** Ar = 4-Cl-C₆H₄, Ar₁ = 4-OCH₃-C₆H₄,
6g: Ar = 4-Cl-C₆H₄, Ar₁ = C₆H₅, **6h:** Ar = 4-Cl-C₆H₄, Ar₁ = 3,4-di-OCH₃-C₆H₃,
6i: Ar = 4-Cl-C₆H₄, Ar₁ = 3,4,5-tri-OCH₃-C₆H₂, **6j:** Ar = Ar₁ = 4-Cl-C₆H₄.

Scheme 2. Synthesis of hydrazide derivatives **5a-f**, pyrrolone derivatives **6a, 6f, 6g-j** and pyridazinone derivatives **7a-f**.

The pyridazinones **7a-f** were prepared by heating at reflux of the appropriate hydrazide derivatives **5a-f** with 6 M hydrochloric acid for 1 h. Also, pyridazinones **7a-f** were obtained directly by heating at reflux of furanones **2a-f** with hydrazine monohydrate in absolute ethanol for 4-24 h.²⁴ The chemical structure of compounds **7a-f** was confirmed by IR, ¹H-NMR and ¹³C-NMR, mass spectra as well as elemental analyses.

2.2. Biology

2.2.1. Anticancer activity

The effect of the tested compounds on the viability of hepatocellular carcinoma HepG2 cells and breast cancer MCF-7 cells were studied using MTT assay after 48 h of incubation. Treatment of hepatocellular carcinoma HepG2 cells and breast cancer MCF-7 cells with gradual concentrations of tested compounds revealed that compounds (**E**)**4b**, **6f**, **7d** and **7f** possessed promising cytotoxic effect on HepG2, with IC₅₀ of 11.47, 7.11, 26.44 and 14.8 μM, respectively, while the other tested compounds showed weak cytotoxic effect on HepG2. Compounds (**E**)**4b** and **6f** possessed promising cytotoxic effect on MCF-7 with IC₅₀ of 18.58 and 19.49 μM, respectively, while the other tested compounds showed weak cytotoxic effect on MCF-7, as shown in Table 1.

Table 1. Collective calculated IC₅₀ (μM) from linear equation of dose response curve for each tested compounds against breast adenocarcinoma MCF-7 and liver carcinoma Hep-G2 cells.

Compound	IC ₅₀ (μM)		Compound	IC ₅₀ (μM)	
	MCF-7	Hep-G2		MCF-7	Hep-G2
2c	49.4	70.34	6a	43.74	37.82
3c	32.64	43	6f	19.49	7.11
E(4b)	18.58	11.47	7b	34.91	103.17
Z(4b)	60.60	>100	7c	47.9	32.4
E(4c)	>100	45.06	7d	37.45	26.44
Z(4c)	39.37	>100	7e	50.53	55.6
E(4d)	66.64	>100	7f	37.12	14.8
E(4e)	40.0	>100	Paclitaxel	0.81	0.73
E(4f)	29.47	37.65			

For more screening of antiproliferative activity, compounds **3c**, **3e**, **3f**, (*E*)**4d**, (*E*)**4f**, (*Z*)**4f**, **5e**, **5f**, **6f**, **7c**, **7e** and **7f** were selected by the National Cancer Institute (NCI) according to the protocol of the Drug Evaluation Branch of the National Cancer Institute²⁵ Bethesda, USA for in vitro anticancer screening. Primary in vitro one dose anticancer assay was performed in full NCI 60 cell lines derived from nine tumor subpanels, including leukemia, melanoma, lung, colon, CNS, ovarian, renal, prostate, and breast cancer cell lines. The selected compounds were added at a single concentration (10^{-5} M) and the culture was incubated for 48 h. End point determinations were made with a protein binding dye sulforhodamine B (SRB). Results for each compound were reported as a mean graph of the percent growth of the treated cells when compared to the untreated control cells. The results of NCI screening for the tested compounds is illustrated in table 2. Compound **3c** exhibited moderate cell growth inhibition activity against renal cancer UO-31 and breast cancer T-47D, also amide **3e** showed moderate cell growth inhibition activity against non-small cell lung cancer NCI-H522 cell line and colon cancer HCT-15. While the chloro amide **3f** showed moderate cell growth inhibition activity against colon cancer HCT-15, prostate cancer PC-3, non-small cell lung cancer NCI-H522 cell line, leukemia K-562, SR, melanoma MDA-MB-435, UACC-62 and breast cancer T-47D, MDA-MB-468 cell line.

On the other hand, the pyrrolone (*E*)**4d** exhibited moderate cell growth inhibition activity against seventeen cell lines; among them leukemia HL-60(TB), SR, non-small cell lung cancer NCI-H522, melanoma M14, SK-MEL-2, prostate cancer PC-3 and breast cancer MCF7, T-47D, MDA-MB-468. A complete cell death was recorded for the melanoma MDA-MB-435 cell line where the growth percent -4.21. Also, pyrrolone (*E*) **4f** exhibited moderate cell growth inhibition activity against fifteen cell lines; among them leukemia SR, K-562, MOLT-4, non-small cell lung cancer NCI-H522, colon cancer HCT-15, CNS cancer U251, melanoma MDA-MB-435, UACC-62, prostate cancer PC-3 and breast cancer MDA-MB-468. In contrast, the cytotoxicity activity falls rapidly when the configuration of **4f** changed from *E* to *Z* against most of the cell lines although the *Z* form exhibited remarkable cell growth inhibition activity against only five tested cell lines.

In addition, the hydrazide **5e** showed significant cell growth inhibition activity against melanoma MDA-MB-435, leukemia SR and breast cancer MDA-MB-468 where the growth percent were 9.68, 26.93 and 27.58, respectively. Compound **5e** revealed moderate cell growth inhibition against fourteen tested cell line; among them leukemia K-

562, non-small cell lung cancer NCI-H460, NCI-H522, breast cancer MCF7, renal cancer UO-31 and prostate cancer PC-3.

Compound **5f** exhibited remarkable cell growth inhibition activity against renal cancer UO-31, breast cancer T-47D and non-small cell lung cancer NCI-H522 only. Also compound **6f** exhibited remarkable cell growth inhibition activity against leukemia HL-60(TB), non-small cell lung cancer HOP-92, NCI-H522, Melanoma UACC-257, renal cancer UO-31 and Breast cancer T-47D.

The pyridazinone **7c** exhibited remarkable cell growth inhibition activity against non-small cell lung cancer NCI-H522, NCI-H226, HOP-62, A549/ATCC, CNS cancer U251, Melanoma UACC-257, UACC-62, renal cancer UO-31 and breast cancer MDA-MB-231/ATCC. A moderate cell growth inhibition was achieved against breast cancer T-47D, MDA-MB-468 and leukemia RPMI-8226 cell lines. Compound **7e** exhibited remarkable cell growth inhibition activity against non-small cell lung cancer NCI-H522, Melanoma UACC-257, renal cancer UO-31, CAKI-1 and breast cancer T-47D while moderate cell growth inhibition was achieved against non-small cell lung cancer HOP-92 cell line only.

Moreover, compound **7f** exhibited moderate cell growth inhibition against breast cancer T-47D and non-small cell lung cancer NCI-H522 cell lines only. A remarkable cell growth inhibition was achieved against leukemia RPMI-8226, MOLT-4, non-small cell lung cancer A549/ATCC, NCI-H226, Melanoma UACC-257, renal cancer UO-31, CAKI-1 and breast cancer MDA-MB-468 cell lines.

The obtained results from NCI screening indicate that the presence of electron withdrawing group on the benzylidene ring of the amide gives better cytotoxicity activity. The *E* form of pyrrolones **4** have good cytotoxicity activity than the open amide form while the *Z* form has less cytotoxicity activity, also the hydrazide have cytotoxicity activity better than the cyclized pyridazinone form if the benzylidene ring have electron donating group, while the reverse is true if the benzylidene ring have electron withdrawing group.

Table 2. % of cell growth inhibition for compounds **3c**, **3e**, **3f**, (*E*)**4d**, (*E*)**4f**, (*Z*)**4f**, **5e**, **5f**, **6f**, **7c**, **7e** and **7f** against different cell lines.

Panel/Cell Line	compound											
	3c	3e	3f	(<i>E</i>)4d	(<i>E</i>)4f	(<i>Z</i>)4f	5e	5f	6f	7c	7e	7f
% of Growth Inhibition												
Leukemia												
CCRF-CEM	1.6	13.9	26.5	26.6	27.4	16.7	26.2	8.5	15.3	10	4	3.9
HL-60(TB)	7.4	15.6	26.2	59.1	23.7	14.6	33.6	9.5	18.8	7.2	6.4	2.3
K-562	0.3	5.4	37.6	48.9	37.8	0	52.8	0.1	0	12.1	0	4.3
MOLT-4	29.8	21.3	27.1	33.2	34.2	1.6	12.5	12.2	2	11.5	12.1	20.3
RPMI-8226	19.5	19.7	24.3	37	29	9.6	19.7	15.6	14.9	30.7	17.7	24.3
SR	13.6	20.7	39.7	54.8	41.4	2.4	73.1	13.1	5.4	17.7	12.5	10.4
Non-Small Cell Lung Cancer												
A549/ATCC	18.8	18.7	15.3	26	15.7	18.3	20	13.4	18.5	24.3	15.5	19.9
EKVX	8.5	6.9	4.4	17.9	4.1	1.8	6	6.7	0	14.4	5.3	12.9
HOP-62	14.6	9.5	17.4	10.3	26.1	9.5	32.6	12.4	16.7	24.5	18.9	14.3
HOP-92	nd ^a	22.6	13.8	35.4	24.7	20.6	30.5	nd	18.8	nd	32.8	nd
NCI-H226	21.5	13.7	26.6	5.1	33.8	11.7	8.3	11.8	12.6	26.9	11.6	23.1
NCI-H23	9	11.1	9.4	14.1	7.3	0	31.1	7.2	4	12	4.8	12.3
NCI-H322M	13.9	18.8	15.5	22.2	19.1	0	18	16.1	10.6	11.7	9.9	3
NCI-H460	0	0	25.6	10	34.7	0	56.4	0	0	5.6	0	0
NCI-H522	19.7	33.1	39.3	48.7	38.2	22.2	47.9	19.5	21.8	28.2	26	30.3
Colon Cancer												
HCT-116	12.4	18.2	17.5	27.5	33.7	5.2	27.7	3.3	7.1	13.2	5.6	6
HCT-15	14	33.2	53	32.4	52.5	0	35.8	0	0.3	12.5	0.3	0
HT29	9.3	1.4	17.9	0	13.3	13.3	0	0	3.3	2.4	0	4.7
KM12	0	0.8	0.3	29.6	1.3	0	26.8	0	0	0	0	0
CNS cancer												
U251	19	4.8	29.4	16.1	35.5	9.4	15.1	8.7	8.4	20.4	12.1	13.7
Melanoma												
LOX IMVI	0	19.7	22.1	19	25.5	0	17.8	0	0	7.6	5.3	3.4
MALME-3M	0	3	20.2	36.5	13.9	7.5	6.6	7.1	0	7.7	0	0
M14	0.2	5.3	5.2	49.5	8.3	2.3	8.5	0	0	3.1	0	0
MDA-MB-435	5.2	0	31.2	104.2	42.9	0	90.3	0	0	6.6	0	3
SK-MEL-2	14	11.7	20.4	48.6	17	0	9.2	11.7	4.6	1.9	0	2.4
SK-MEL-28	0	0	8.8	20.1	10.9	0	24.3	0	0	0	0	0
SK-MEL-5	11.3	15.8	6.6	33.8	9.5	0.1	25	0	6.5	11.5	5.9	10.2
UACC-257	24.4	5.9	29.3	28.3	34.2	23.1	18.5	15	19.6	27.7	18.9	23.5
UACC-62	23.1	4	32.7	36.1	38.9	10	24.2	16.8	9.1	20	11.1	16.9
Ovarian Cancer												
IGROV1	20.5	16.1	13.7	22.5	19.4	0.4	17.4	15.4	5.6	9.4	10.2	7.2
OVCAR-8	14.6	7.2	17.7	29.1	16.6	8.2	19.3	11.2	8.6	13.6	9.3	9.1
NCI/ADR-RES	5.8	14.1	10.9	20.1	8.1	0	25.2	0	0	8.6	5.9	5.2
SK-OV-3	12.4	3.1	20.7	26.2	26.8	11.9	20.1	15.7	14.9	13.8	12.9	5.5
Renal Cancer												
CAKI-1	25.2	20.5	12.6	6.8	10	7	22.1	3.9	6.2	18	20.5	22.3
TK-10	20.4	17.7	27.3	14.7	16.5	13.3	0	0	3.4	0	0	8.1
UO-31	38.3	28.1	24	31.6	25.8	4	32.1	23.3	21.3	26	24.2	27.3
Prostate Cancer												
PC-3	15	19.2	43.6	47.8	48.3	20.6	32.7	0	13.9	16.8	7.9	8.4
Breast Cancer												
MCF7	16.5	23.8	13.9	37.2	14.7	0	52.1	9.8	13.2	1.5	0	8
MDA-MB231/ATCC	13	9.5	18.7	6.3	22.4	0.1	34.6	12.7	0.1	22.2	10.6	19.2
HS 578T	5.5	17.5	13.6	25.2	12.9	0	0	2.2	0	8.6	2.4	0
BT-549	0	17.6	0	29.6	0	0	36.3	0	0	15.4	7.2	0
T-47D	46.7	29.3	34.7	31.1	36.1	16.2	33	22	29.4	39.5	22.6	35.4
MDA-MB-468	16.5	18	30.3	46.3	37.5	13.3	72.4	0.7	13.6	31.3	7.9	27.3

nd^a: not detected

2.2.2. Immunofluorescence localization of tubulin in liver cancer cells

The localization of tubulin was explored in Hep-G2 cell line after treatment with selected promising compounds that revealed an inhibitory effect in tubulin as indicated by ELISA. Cells were treated with 25 $\mu\text{g}/\text{mL}$ of each compound for 48 h, and then submitted to immunofluorescence labeling and analysis under Apo time fluorescence microscope.

Compounds (**E**)**4b**, **6f**, **7d** and **7f** showed a variable promising inhibitory effect of cellular localization of tubulin (**Fig. 3**), as concluded from the inhibition of the fluorescence intensities.

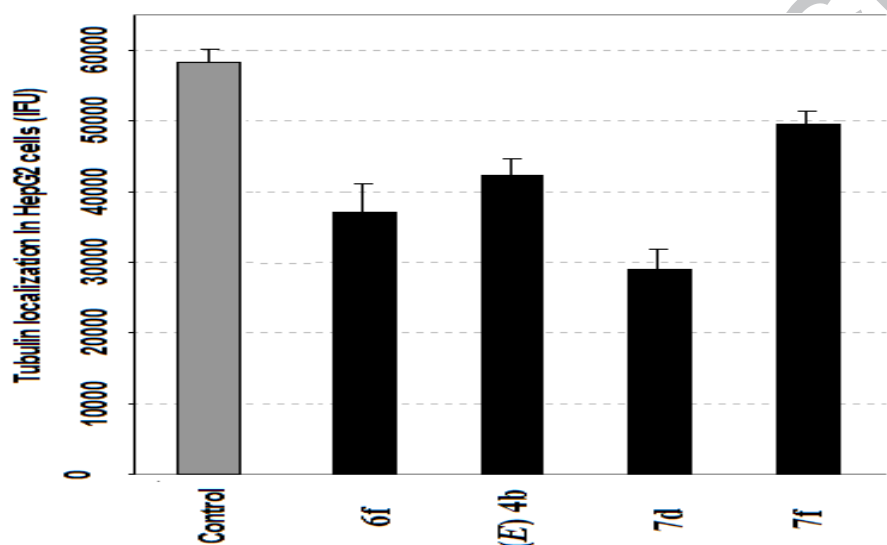


Fig. 3. Fluorescence intensity (IFU) of tubulin localization in HepG-2 cells after treatment for 48 h by tested compounds. Grey bar represent control cells.

Treatment with compounds (**E**)**4b**, **6f**, **7d** and **7f** resulted in a high degree of cellular cytotoxicity and malformed cellular structure with shrunk nuclei. Abnormal cytoplasm/ nucleus proportion with reduced cytoplasm and abnormal diminished tubulin expression pattern. The cell-cell microtubules mesh disappeared, although the cells possessed relatively high tubulin, but not distributed in a normal cellular distribution pattern (**Fig. 4**).

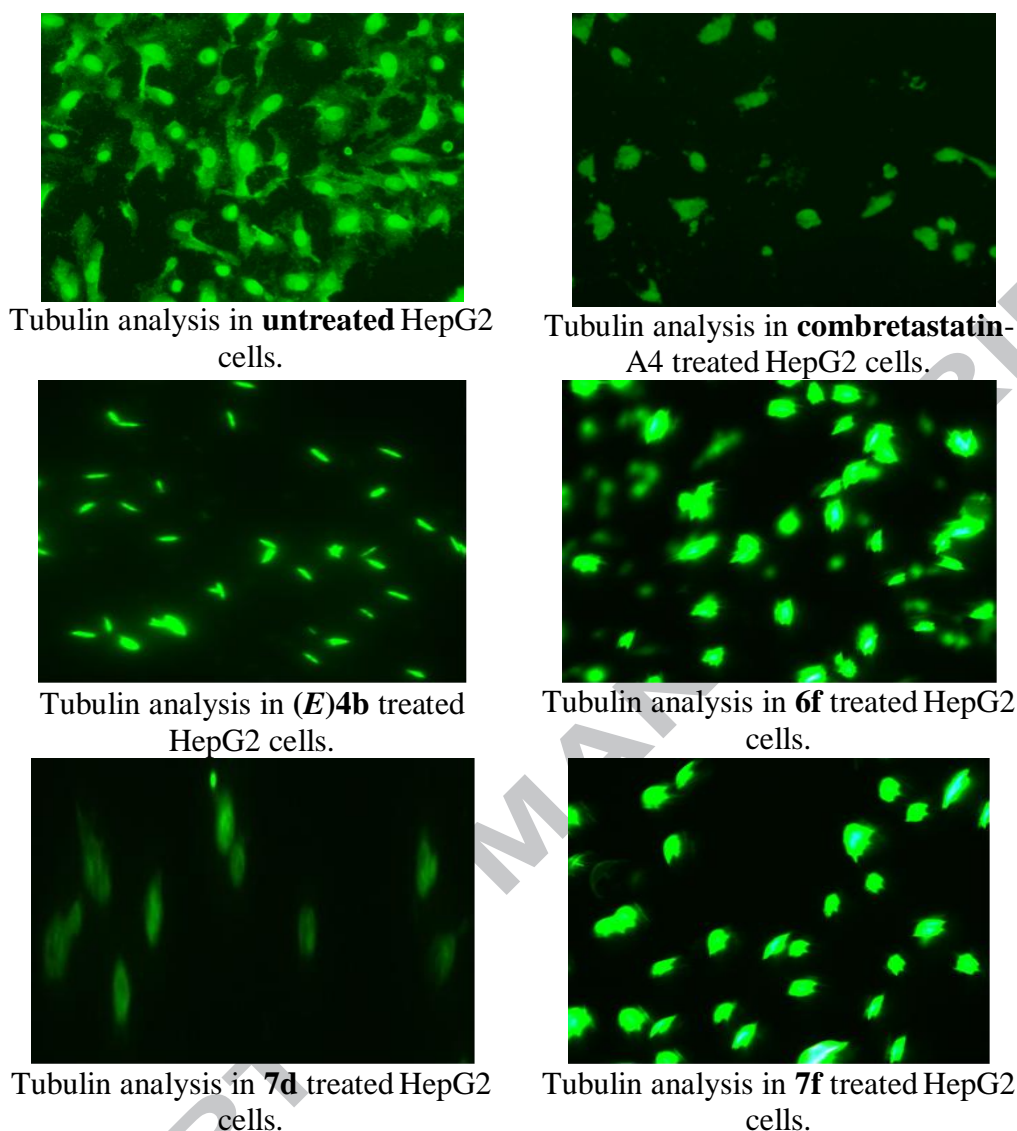


Fig. 4. Fluorescence intensity (IFU) of tubulin localization in HepG-2 cells after treatment with combretastatin-A4, (**E**)4b, **6f**, **7d** and **7f** for 48 h compared to control cells (photo X 200) as captured by Apotome fluorescence microscope.

2.2.3. Cell cycle analysis

To explore the alteration in the cell cycle phases after treatment with the active cytotoxic compounds (**E**)4b, the cells were subjected to flow cytometry analysis. The analysis indicated that in HepG2 cells treated with (**E**)4b induced G2/M arrest of HepG2 cells and S-phase arrest, where a large proportion of cells were accumulated in S- and G2/M-phase ($P < 0.05$). HepG2 cells treated with (**E**)4b showed a predominated growth

arrest at the S- phase higher than that of G2/M-phase ($P < 0.01$) as compared with control cells, where the S-phase progression of HepG2 cells was considerably delayed (**Fig. 5**).

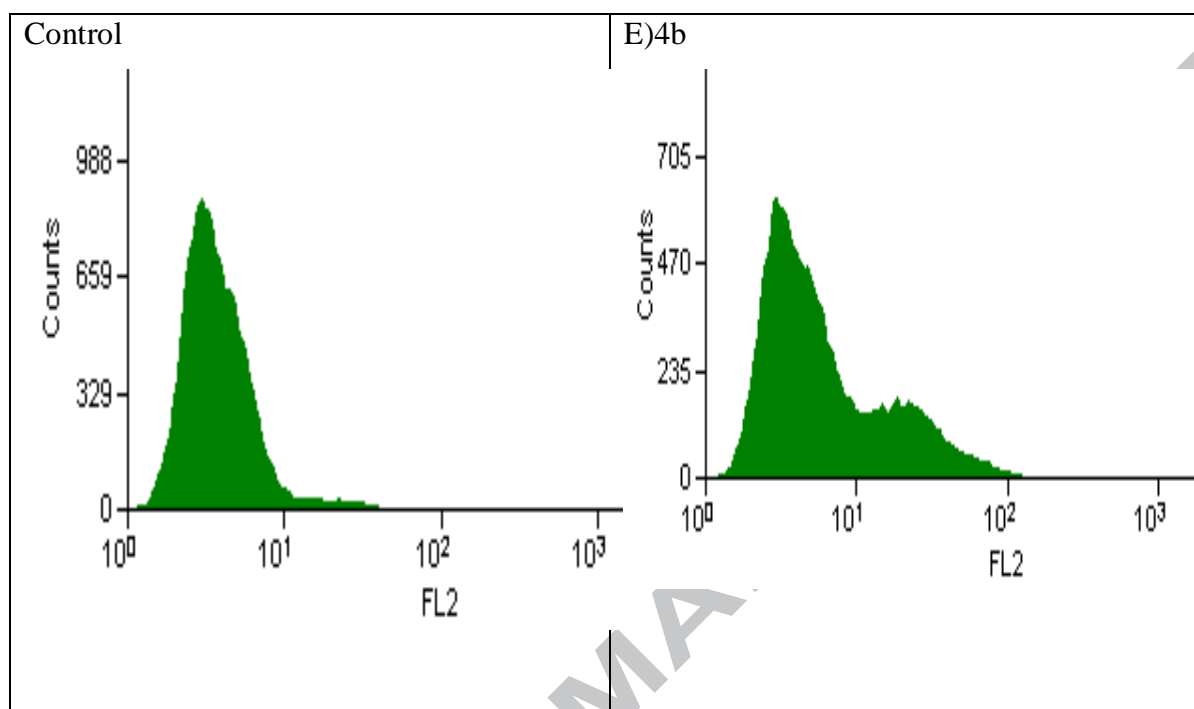


Fig.5. Flow cytometry analysis of HepG2 cells treated with (**E**)**4b** showed a predominated growth arrest at the S- phase higher than that of G2/M-phase ($P < 0.01$) as compared with control cells, where the S-phase progression of HepG2 cells were considerably delayed.

2.3. Docking of the target molecules on 1SA0, Tubulin-Colchicine: Stathmin-like domain complex.

Molecular modeling study was carried out for the synthesized compounds including **3b**, **3f**, (**E**)**4b**, (**E**)**4c**, (**E**) **4d**, (**E**)**4e**, (**E**)**4f**, (**Z**)**4b**, (**Z**)**4c**, (**Z**)**4f**, **5d**, **5f**, **6a**, **6f-j** and **7a-f**, DAMA-Colchicine and combretastatin A-4 in the active colchicine binding site of tubulin polymerase enzyme using Molecular Operating Environment (MOE®) version 2014.09. DAMA-Colchicine was bound in the active site through two H-bond interactions between the ligand with Lys352 and Ala317, also there are strong hydrophobic interactions between the ligand and Lys352, Leu255, Asn258, Leu248, Lys254 and Ala316 as reported in the literature.²⁶ On the other hand, Combretastatin A-4 showed only one hydrogen bond between the hydroxyl group of the ligand and Lys-352. In addition, there are strong hydrophobic interactions between the ligand and Lys352, Ala316, Leu255, Asn258 and Leu248, while in the literature binding of CA-4 on 1AS0 revealed formation

of two hydrogen bonds with Cys241 and strong hydrophobic interaction with Leu242, leu255, Ala250, Ala 318, Ala316, Lys352, Ile378 and Val 315.²⁷

All the tested compounds showed inhibition of β -subunit of tubulin as the binding free energy (dG) values of them above or around (-10) Kcal/mole (**Table 3**). The data in **Table 2** showed a rough correlation between the dG values of the target compounds and their activity (expressed as IC₅₀ values against liver cancer cells). All compounds have dG value as Combretastatin A-4 dG value.

Table 3. Interaction energies of tested compounds, DAMA-Colchicine and combretastatin A-4 in the active site β -subunit of tubulin.

Compound	dG Kcal/mole	Compound	dG Kcal/mole
DAMA-Colchicine	-12.04	5f	-10.74
Combretastatin A-4	-10.01	6a	-11.07
3b	-10.74	6f	-11.16
3f	-10.26	6g	-12.81
E(4b)	-10.45	6h	-11.86
E(4c)	-12.96	6i	-11.51
E(4d)	-10.69	6j	-11.01
E(4e)	-10.46	7a	-9.94
E(4f)	-11.29	7b	-10.13
Z(4b)	-11.16	7c	-10.75
Z(4c)	-10.94	7d	-10.18
Z(4f)	-10.22	7e	-10.74
5d	-10.79	7f	-9.99
5f	-10.74		

Binding modes of tested compounds with tubulin binding site.

Molecular docking simulation of the amide **3b** (Fig. 6) into tubulin active site, revealed presence of one hydrogen bond between the hydroxyl group of the ligand and Lys-352 at distance 3Å like combretastatinA-4, in addition to several hydrophobic interactions between the ligand and critical amino acid residues including Leu248, Lys254, Leu255, Lys352 and Asn258 like DAMA-colchicine.

On the other hand, molecular docking simulation of the amide **3f** revealed one hydrogen bond between the ligand but with Asn-258 and pi-cation interaction between halophenyl ring of the ligand and Lys352. Also there are several hydrophobic interactions between the ligand and Leu248, Leu255, Lys352, Ala316, Ile347, Asn349 and Asn258.

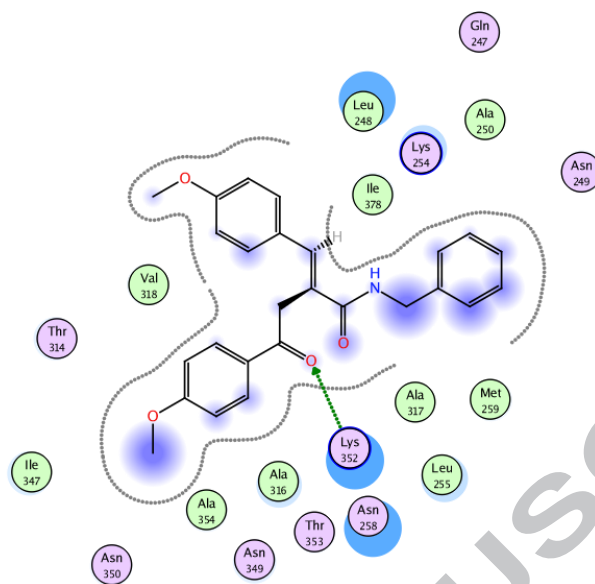


Fig. 6. 2D representation of docking of **3b** in β -subunit of tubulin.

Molecular docking simulation of the cyclized form of the amide **3b** the pyrrolone **E(4b)** (Fig.7, 8) which showed inhibitory activity against MC7 and HepG2 cells revealed presence of pi-cation interaction between the ligand and Lys-352 instead of hydrogen bond in case of its amide **3b**, in addition to several hydrophobic interactions between the ligand and critical amino acid residues including Leu248, Lys254, Leu255, Ala316, Lys352 and Asn258 like compound **3b**.

It is reasonable to note the presence of hydrogen bond or pi-cation interaction with Lys352 at distance like that of compound **E(4b)** around 3.81Å along with strong hydrophobic interaction in the active site is essential for activity, therefore the lack of activity in compound **E(4c)** due to the absence of interaction with Lys352. Compounds **E(4d)** and **E(4f)** showed inhibitory activity because of presence of interaction with Lys352. On the other hand compound **E(4e)** lacks activity due to it has less hydrophobic interaction in the binding site although it have pi-cation interaction with Lys352 at 3.79Å.

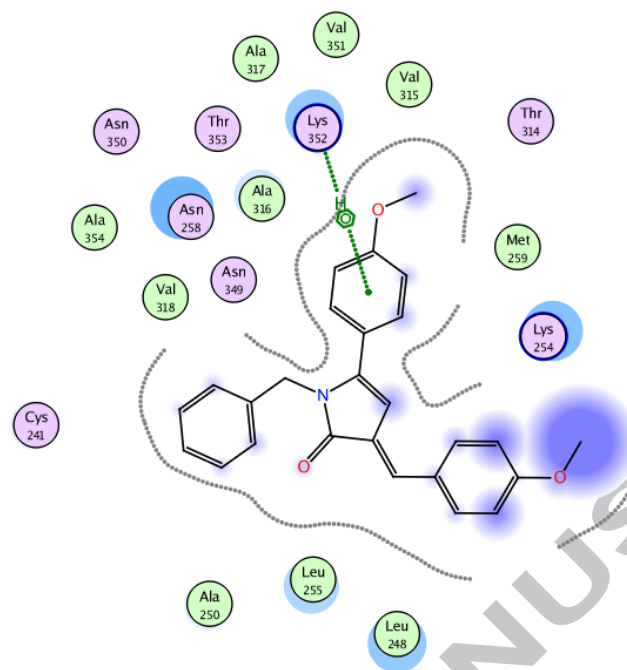


Fig. 7. 2D representation of docking of **E 4b** in β -subunit of tubulin.

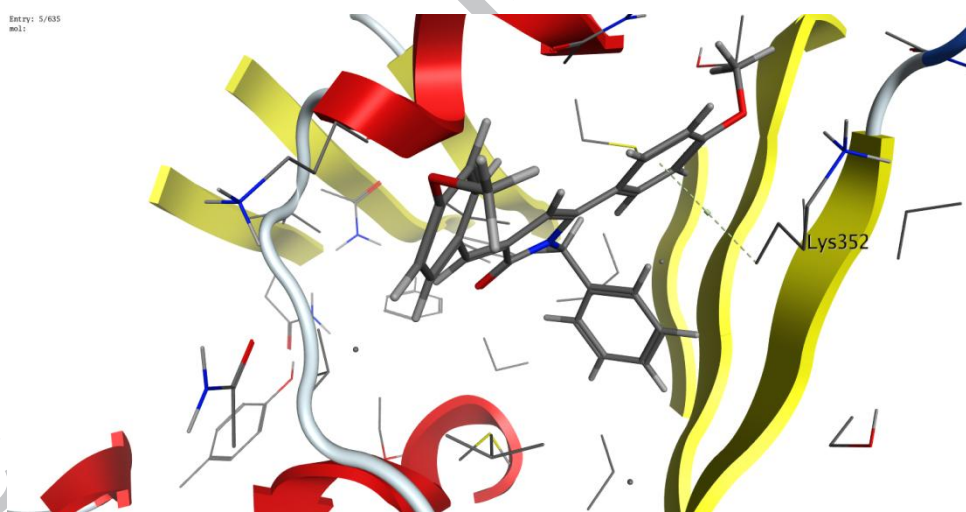


Fig. 8. Docking of **E(4b)** into the tubulin active site obtained from the crystal structure of **E(4b)** complex.

Regarding the stereochemistry effect in binding on 1AS0, Molecular docking simulation of compound **E4b** and **Z4b** revealed that the **E** form have strong hydrophobic interaction with the critical amino acids in the binding site than that formed in case of **Z** form, also the **Z4b** (Fig.9) lacks the pi-cation interaction with Lys352 as confirmed with inhibitory activity. Also molecular docking simulation of compounds **Z4c** and **Z4f**

revealed absence of pi-cation interaction with Lys 352 or its presence but at distance 4.6Å respectively.

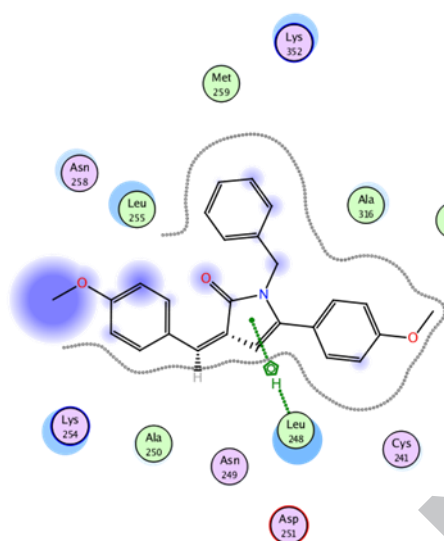


Fig. 9. 2D representation of docking of **Z (4b)** in β -subunit of tubulin.

Also, molecular docking simulation of hydrazide **5d** (Fig.10) revealed presence of hydrogen bond and pi-cation interaction between the ligand with Asn258 and Lys352 respectively, in addition to hydrophobic interaction between the ligand and Leu248, Leu255, Cys241, Lys352, Ala316 and Asn258, while hydrazide **5f** was showed two hydrogen bond interactions between the ligand and Cys241 and Lys254, in addition to less hydrophobic interactions in the binding site than compound **5d**.

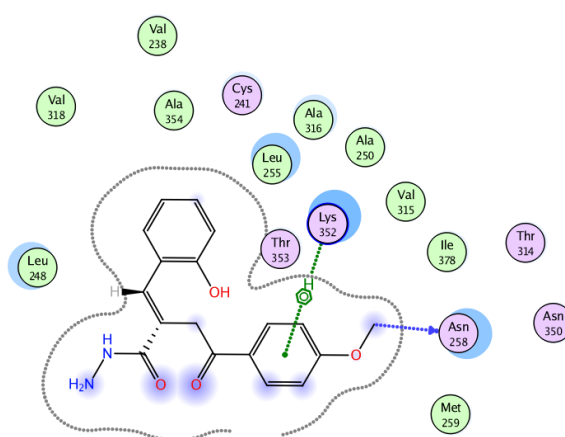


Fig. 10. 2D representation of docking of **5d** in β -subunit of tubulin.

Molecular docking simulation of compound **6a** was showed no interaction with the active site of tubulin these may be due to the steric effect as confirmed with the biological activity., while binding of compounds **6f** (Fig.11) which is the most active compound against Hep-G2 carcinoma, revealed presence of one pi-cation interaction between the ligand and Asn258 for **6f** and hydrophobic interaction between the ligand and Leu248, Leu255, Lys254 Lys352 and Asn258. This means presence of pi-cation or hydrogen bond interaction with Asn258 along with strong hydrophobic interaction with critical amino acid residues in the binding side produce active compounds. Compound **6i** expected to have similar activity as pyrrolone **6f** because it has similar interaction like **6f** except formation of hydrogen bond with Asn258 instead of pi-cation interaction. On the other hand compounds **6g**, **6h** expected to have good inhibitory activity through its pi-cation interaction with Lys 352 with distance 3.73Å and 4.1Å as pyrrolone **E4b**, in addition to the presence of hydrophobic interactions. Compounds **6j** is expected to have less inhibitory activity than pyrrolone **6f** because of their formation of pi-cation interaction with Lys352 with distance 4.98Å.

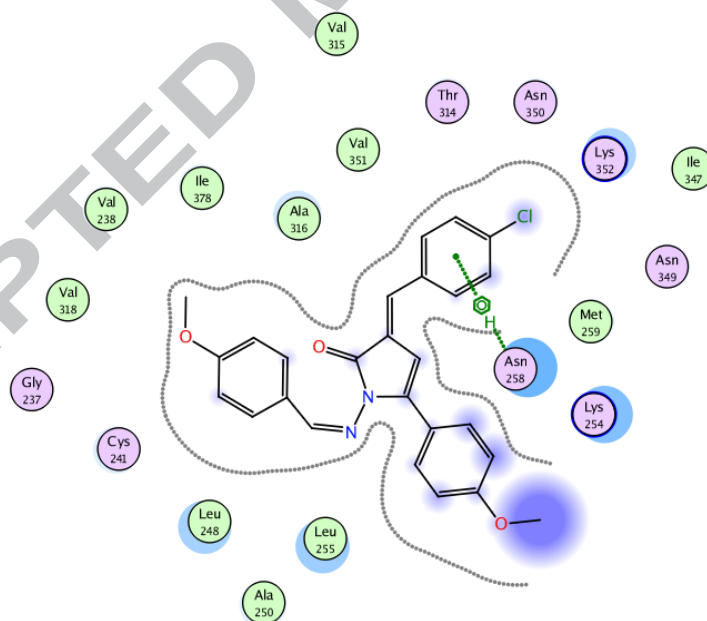


Fig. 11. 2D representation of docking of **6f** in β -subunit of tubulin.

Regarding the pyridazinones **7a** and **7e**, their mode in binding may reflect that they have no or little inhibitory activity because they have weak hydrophobic interaction, also its binding revealed formation of pi-cation interaction with Lys352 at distance 4.51Å and 3.11Å, respectively. Also compound **7c** have weak inhibitory activity because it has

weak hydrophobic interaction in spite of its formation of pi-cation interaction with Lys352 at distance 3.70Å.

On the other hand, pyridazinones **7d** (Fig.12) and **7f** which were shown moderate inhibitory activity against Hep-G2 carcinoma, revealed presence of hydrophobic interaction, in addition to hydrogen bond interaction with Cys241 at distance 3.88Å in case of **7d** while formation of pi-cation interaction with Lys352 at distance 3.89Å in case of **7f**. This means the contribution of inhibitory activity of binding with Lys 352 is more than that of Cys241 because of the inhibitory effect of **7f** more than that of **7d**. Again here the distance in binding is critical issue as well as the binding with critical amino acid, therefore in case of compound **7b** although it form four interaction with the binding site, three of them H bond of the ligand with Cys 241 at distance 3.17Å, Ala 250 & Asp 251 and the fourth one is pi-cation between the ligand and Lys 254 but it has very weak inhibitory activity.

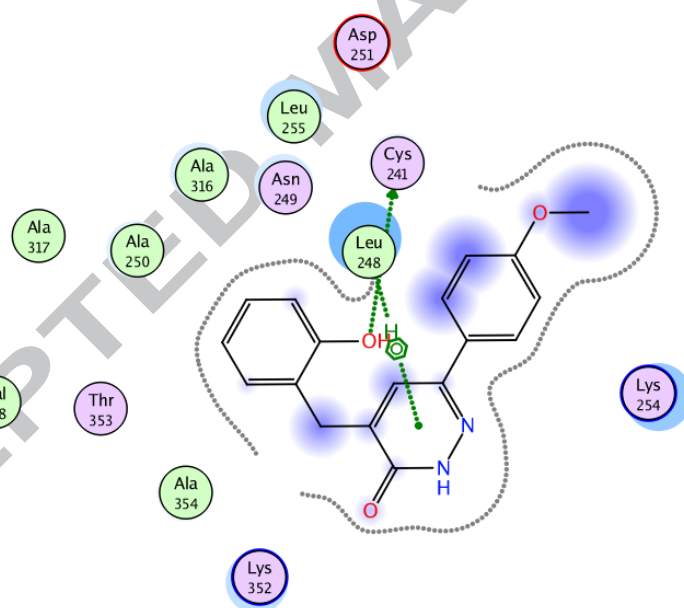


Fig. 12. 2D representation of docking of **7d** in β -subunit of tubulin.

3. EXPERIMENTAL

3.1: Chemistry

Melting points was determined using Stuart electrothermal melting point apparatus and were uncorrected. The IR Spectra were carried out using Shimadzu IR-408 spectrophotometer, KBr pellets; Bruker Tensor 27 or Nicolet iS5 (ATR) FT-IR spectrometer. For ^1H NMR Spectra: Varian Germany NMR spectrophotometer (200 MHz)

or Varian Mercury VX-300 NMR spectrometer (300 MHz) or Bruker apparatus (DRX 400 MHz); or JEOL-JNM-LA-400 FT-spectrometer (400 MHz); chemical shift (δ) in ppm relative to TMS ($\delta = 0$ ppm) as internal standard and CDCl_3 or $\text{DMSO}-d_6$ as a solvent. Coupling constant (J) in Hz, geminal coupling (2J), vicinal coupling (3J) and the signals are designated as follows: s, singlet; d, doublet; t, triplet; q, quartet; m, multiplet. For ^{13}C NMR Spectra: Bruker 300 MHz NMR spectrometer (75 MHz), or Bruker apparatus (100 MHz); For EI-MS: Shimadzu GC/ MS- QP5050A, or Shimadzu Qp-2010 Plus. for Elemental analyses: Vario EL III German CHN Elemental analyzer model, or GmbH Vario EL V2.3 CHN Elemental analyzer model, *X-ray crystallography: using maXus, X-ray lab, National Research Centre, Dokki, Giza, Egypt.* Chemicals and solvents used in the preparation of the target compounds are of commercial grade, and purchased from Alfa Aesar, Cambrian chemicals, Aldrich, Acros Organics, Fluka, Merck, and El-Nasr pharmaceutical chemicals companies. Chemicals and solvents were used without purification. The reactions progresses were monitored using TLC (Kieselgel 60 F₂₅₄ precoated plates, E. Merck, Darmstadt, Germany), the spots were detected by exposure to UV lamp. Compounds **1**²⁸, **2a**²⁹, **2b**²⁹, **2c**³⁰, **2d**³¹, **2e**³², **2f**³⁰, **3a**³³ and **4a**³³ are prepared as in the literature.

3.1.1: General procedure for Synthesis of *N*-benzyl-2-benzylidene-4-oxo-4-(4-methoxyphenyl)butanamides 3a-f.

Heating at reflux the appropriate furanone derivatives **2a-f** (0.003 mol) and benzylamine (0.004 mol, 0.43 g) in dry benzene for 5 h. The mixture leave to cool and the obtained crystals were filtered off, washed with dry benzene.

3.1.1.1: (*E*)-*N*-Benzyl-2-benzylidene-4-(4-methoxyphenyl)-4-oxobutanamide 3a.³³

White crystal ; (1.04 g, 90.4% yield); mp 129-131°C; IR (KBr) ν_{max} = broad band 3264 cm^{-1} (NH), 1670 cm^{-1} (C=O benzoyl), 1636 cm^{-1} (C=O amide); ^1H -NMR (400 MHz, CDCl_3) δ (ppm) = 3.82 (s, 3H, OCH_3), 4.84 (s, 2H, N-CH_2), 6.21 (s, 1H, olefinic H_a), 6.86 (d, 2H, $J = 8.0$ Hz, ArH), 7.09 (d, 2H, $J = 8.0$ Hz, ArH), 7.18-7.22 (m, 2H, ArH), 7.24-7.28 (m, 3H; 2H, ArH and 1H, olefinic H_b , enol tautomer C), 7.34-7.39 (m, 2H, ArH), 7.42 (d, 2H, $J = 6.8$ Hz, ArH), 7.48 (s, 1H, NH), 7.64 (d, 2H, $J = 6.8$ Hz, ArH).

3.1.1.2: (E)-N-Benzyl-2-(4-methoxybenzylidene)-4-(4-methoxyphenyl)-4-oxobutanamide 3b.

White crystals; (0.93 g, 74.3% yield); mp = 127-129°C; IR (KBr) ν_{\max} = broad band 3302 cm^{-1} (NH and OH), 1673 cm^{-1} (C=O benzoyl), 1645 cm^{-1} (C=O amide); $^1\text{H-NMR}$ (300 MHz, CHCl_3) δ (ppm) = 3.37 (s, 2H, COCH_2), 3.80 (s, 3H, OCH_3), 3.81 (s, 3H, OCH_3), 3.97 (s, 1H, OH) 4.08 (d, 1H, $^2J=15.0$ Hz, N- CH_2), 4.70 (d, 1H, $^2J=15.0$ Hz, N- CH_2), 6.81 (s, 1H, olefinic H_a , enol tautomer **B**), 6.84 (d, 2H, $J=9.0$ Hz, ArH), 7.17-7.28 (m, 2H, ArH), 7.30 (d, 2H, $J=9.0$ Hz, ArH), 7.34-7.36 (m, 4H, ArH), 7.37-7.38 (m, 2H, ArH), 7.48 (s, 1H, ArH); $^{13}\text{C NMR}$ (100 MHz, CDCl_3) δ (ppm) = 169.7, 160.0, 159.4, 138.2, 134.2, 131.4, 131.4, 128.8, 128.2, 128.0, 127.2, 127.1, 125.7, 114.2, 113.6, 90.5, 55.3, 55.3, 45.4, 43.8; EI-MS (70 eV) m/z (%) 415 (M^+ , 14), 397 (100), 306 (35), 291 (15), 277 (2), 247 (4), 171 (4), 159 (3), 135 (78), 91 (76), 83 (27), 71 (44). Anal. Calcd. For $\text{C}_{26}\text{H}_{25}\text{NO}_4$ (415.18): C, 75.16; H, 6.06; N, 3.37. Found: C, 75.35; H, 6.09; N, 3.51.

3.1.1.3: (E)-N-Benzyl-4-(4-methoxyphenyl)-4-oxo-2-(3,4,5-trimethoxybenzylidene)-butanamide 3c.

White crystals; (1.04 g, 77.5% yield); mp = 176-178°C; IR (KBr) ν_{\max} = broad band 3284 cm^{-1} (NH and OH), 1670 cm^{-1} (C=O benzoyl), 1643 cm^{-1} (C=O amide); $^1\text{H-NMR}$ (300 MHz, CDCl_3) δ (ppm) = 3.83 (s, 3H, OCH_3), 3.90 (s, 6H, 2OCH_3), 3.91 (s, 3H, OCH_3), 4.84 (s, 2H, N- CH_2), 6.13 (s, 1H, olefinic H_a), 6.87-6.9 (m, 4H, ArH), 7.07-7.10 (m, 3H, ArH), 7.23-7.26 (m, 5H; 4H, ArH and 1H, olefinic H_b , enol tautomer **C**), 7.41 (s, 1H, NH); EI-MS (70 eV) m/z (%) 475 (M^+ , 17), 460 (9), 457 (100), 337 (3), 321 (6), 277 (15), 247 (2), 159 (2), 135 (67), 107 (11), 106 (15), 91 (76), 83 (5). Anal. Calcd. For $\text{C}_{28}\text{H}_{29}\text{NO}_6$ (475.20): C, 70.72; H, 6.15; N, 2.95. Found: 70.83; H, 6.22; N, 3.02.

3.1.1.4: (E)-N-Benzyl-2-(2-hydroxybenzylidene)-4-(4-methoxyphenyl)-4-oxobutanamide 3d.

White crystal; (0.5 g, 41.5% yield); mp = 178-180°C; IR (KBr) ν_{\max} = broad band 3356 cm^{-1} (NH and OH), 1681 cm^{-1} (C=O benzoyl), 1649 cm^{-1} (C=O amide); $^1\text{H-NMR}$ (400 MHz, CDCl_3) δ (ppm) = 3.35 (s, 2H, COCH_2 , enol tautomer **C**), 3.84 (s, 3H, OCH_3), 4.20 (d, 1H, $^2J=9.0$ Hz, N- CH_2 , enol tautomer **B**), 4.87 (s, 1H, OH), 4.89 (d, 1H, $^2J=9.0$ Hz, N- CH_2), 6.23 (s, 1H olefinic H_a), 6.87 (d, 2H, $J=8.0$ Hz, ArH), 6.96 (d, 2H, $J=8.0$ Hz, ArH), 7.15-7.24 (m, 2H; 1H, ArH, 1H and 1H, olefinic H_b), 7.26-7.35 (m, 2H, ArH),

7.37-7.47 (m, 2H; 1H, ArH, 1H, OH), 7.67-7.69 (m, 2H, ArH), 8.06-8.34 (m, 2H, ArH), 8.36 (d, 1H, $J = 8.0$ Hz, ArH), 9.30 (s, 1H, NH); EI-MS (70 eV) m/z (%) 401 (M^+ , 1), 383 (0.38), 294 (1), 159 (3), 135 (100), 107 (6), 92 (8), 83 (1), 77 (21). Anal. Calcd. For $C_{25}H_{23}NO_4$ (401.16): C, 74.79; H, 5.77; N, 3.49. Found: 74.88; H, 5.82; N, 3.54.

3.1.1.5: (E)-N-Benzyl-2-(4-hydroxy-3-methoxybenzylidene)-4-(4-methoxyphenyl)-4-oxobutanamide 3e.

Pale yellow crystals; (0.87 g, 67.3% yield); mp = 162-164°C; IR (KBr) ν_{max} = broad band 3401 cm^{-1} (NH and OH), 1666 cm^{-1} (C=O benzoyl), 1644 cm^{-1} (C=O amide); 1H -NMR (300 MHz, $CDCl_3$) δ (ppm) = 3.84 (s, 3H, OCH_3), 3.93 (s, 3H, OCH_3), 4.85 (s, 2H, N- CH_2), 6.30 (s, 1H, olefinic H_a), 6.87 (d, 2H, $J = 9.0$ Hz, ArH), 6.95 (d, 1H, $J = 8.1$ Hz, ArH), 7.08-7.11 (m, 2H, ArH), 7.14-7.15 (m, 1H, ArH), 7.20- 7.24 (m, 3H; 2H, ArH and 1H, olefinic H_b , enol tautomer **C**), 7.25- 7.29 (m, 4H; 3H, ArH and OH), 7.37 (s, 1H, ArH), 7.43 (s, 1H, NH). Anal. Calcd. For $C_{26}H_{25}NO_5$ (431.17): C, 72.37; H, 5.84; N, 3.25. Found: C, 72.54; H, 5.90; N, 3.21.

3.1.1.6: (E)-N-Benzyl-2-(4-chlorobenzylidene)-4-(4-methoxyphenyl)-4-oxobutanamide 3f.

White crystals; (0.93 g, 74.0% yield); mp = 167-168°C; IR (KBr) ν_{max} = broad band 3309 cm^{-1} (NH and OH), 1690 cm^{-1} (C=O benzoyl), 1645 cm^{-1} (C=O amide); 1H -NMR (400 MHz, $CDCl_3$) δ (ppm) = 3.82 (s, 3H, OCH_3), 4.84 (s, 2H, N- CH_2), 6.14 (s, 1H, olefinic H_a , enol tautomer **C**), 6.86 (d, 2H, $J = 8.40$ Hz, ArH), 7.08 (d, 2H, $J = 8.00$ Hz, ArH), 7.19-7.24 (m, 3H, ArH), 7.25-7.27 (m, 3H, 2H, ArH and 1H, olefinic H_b), 7.36 (d, 2H, $J = 8.0$ Hz, ArH), 7.40 (s, 1H, NH), 7.56 (d, 2H, $J = 8.4$ Hz, ArH), 1H -NMR (400 MHz, $CDCl_3$) δ (ppm) = 3.36 (s, 2H, $COCH_2$), 3.81 (s, 3H, OCH_3), 3.94 (s, 1H, OH) 4.20 (d, 1H, $^2J = 15.0$ Hz, N- CH_2), 4.71 (d, 1H, $^2J = 15.0$ Hz, N- CH_2), 6.79-6.82 (m, 2H; 1H, ArH and 1H, olefinic H_a , enol tautomer **B**), 7.10-7.12 (m, 3H, ArH), 7.15-7.17 (m, 3H, ArH), 7.26-7.41 (m, 5H, ArH), 7.42 (s, 1H, ArH); EI-MS (70 eV) m/z (%) 419 (M^+ , 12), 401 (100), 310 (13), 282 (10), 281 (5), 275 (38), 247 (4), 232 (22), 172 (2), 158 (3), 135 (87), 91 (69), 83 (3), 77 (9). Anal. Calcd. For $C_{25}H_{22}ClNO_3$ (419.13): C, 71.51; H, 5.28; N, 3.34. Found: C, 71.72; H, 5.25; N, 3.40.

3.1.2: General procedure for the synthesis of (E)-1-benzyl-3-benzylidene-5-(4-methoxyphenyl)-1H-pyrrol-2(3H)-ones 4a-f.

Method A:-

Heating at reflux of the appropriate amide **3** (0.003 mol) in 6 M hydrochloric acid (20mL) for 1 h, then The contents were left to cool and the obtained solid mass was filtered off, washed with water and crystallized from ethanol to give compounds (*E*) **4a-f**.

Method B:-

Heating at reflux a mixture of the appropriate amide **3** (0.003 mol) and hydroxylamine hydrochloride (0.003 mol) in ethanol for 7 h, the reaction mixture was allowed to cool. The obtained crystals were filtered off and crystallized from ethanol to give compounds (*E*) **4a-f**.

3.1.2.1: (E)-1-Benzyl-3-benzylidene-5-(4-methoxyphenyl)-1H-pyrrol-2(3H)-one 4a³³

Red crystals; (method A; 0.74 g, 67.0% yield, method B; 0.84 g, 76.0% yield); mp = 142-143°C; IR (KBr) ν_{\max} = 1694 cm^{-1} (C=O of pyrrolone); ¹H-NMR (300 MHz, CDCl₃) δ (ppm) = 3.84 (s, 3H, OCH₃), 4.85 (s, 2H, N-CH₂), 6.21 (s, 1H, olefinic H), 6.87 (d, 2H, *J* = 8.7 Hz, ArH), 7.01 (d, 2H, *J* = 8.1Hz, ArH), 7.23-7.28 (m, 5H, ArH), 7.38-7.43 (m, 3H, ArH), 7.50 (s, 1H, H-4 pyrrolone ring), 7.65 (d, 2H, *J* = 8.1 Hz, ArH); ¹³C NMR (75 MHz, CDCl₃) δ (ppm) = 160.7, 160.4, 149.7, 138.1, 136.3, 136.1, 132.4, 130.5, 130.4, 129.6, 129.1, 128.8, 127.4, 127.3, 114.8, 114.3, 100.2, 56.6, 44.8.

3.1.2.2: (E)-1-Benzyl-3-(4-methoxybenzylidene)-5-(4-methoxyphenyl)-1H-pyrrol-2-(3H)-one 4b.

Red crystals; (method A; 0.65 g, 54.9% yield, method B; 0.94 g, 78.8% yield.); mp = 103-105°C; IR (KBr) ν_{\max} = 1690 cm^{-1} (C=O of pyrrolone); ¹H-NMR (400 MHz, CDCl₃) δ (ppm) = 3.77 (s, 3H, OCH₃) , 3.78 (s, 3H, OCH₃), 4.82 (s, 2H , N-CH₂), 6.18 (s, 1H, olefinic H), 6.68 (d, 2H, *J* = 8.8 Hz, ArH), 6.94 (d, 2H, *J* = 9.0 Hz, ArH), 7.07 (d, 2H, *J* = 9.0 Hz, ArH), 7.16-7.21(m, 2H, ArH) , 7.23-7.27 (m, 3H, ArH) , 7.46 (s, 1H, pyrrolone), 7.62 (d, 2H, *J* = 8.8 Hz, ArH); ¹³C NMR (75 MHz, CDCl₃) δ (ppm) = 160.5, 160.1, 159.9, 148.2, 137.7, 131.9, 131.8, 129.3, 129.2, 128.4, 128.3, 126.9, 125.9, 114.6, 113.4, 112.5, 99.9, 55.6, 55.5, 48.6; EI-MS (70 eV) *m/z* (%) 397 (M⁺, 100), 306 (36), 291 (18), 290 (3), 263 (23), 260 (4), 189 (7), 173 (1), 170 (1), 135 (29), 108 (1), 107 (4), 94 (1), 91

(68), 81 (1), 82 (1), 77 (9), 65 (14). For $C_{26}H_{23}NO_3$ (397.17): C, 78.57; H, 5.83; N, 3.52. Found: C, 78.74; H, 5.88; N, 3.59.

3.1.2.3: (E)-1-Benzyl-5-(4-methoxyphenyl)-3-(3,4,5-trimethoxybenzylidene)-1H-pyrrol-2-(3H)-one 4c.

Red crystals; (method A; 0.75 g, 55.0% yield, method B; 0.69 g, 50.0% yield); mp = 101-103°C; IR (KBr) ν_{\max} = 1687 cm^{-1} (C=O of pyrrolone); 1H -NMR (400 MHz, $CDCl_3$) δ (ppm) = 3.81 (s, 3H, OCH_3), 3.89 (s, 3H, OCH_3), 3.91 (s, 6H, $2OCH_3$), 4.84 (s, 2H, N- CH_2), 6.15 (s, 1H, olefinic H), 6.24 (s, 2H, ArH), 6.89 -7.02 (m, 5H, ArH), 7.08 (d, 2H, J = 6.4 Hz, ArH), 7.20 -7.40 (m, 2H, ArH), 7.41 (s, 1H, H-4 pyrrolone ring). Anal. Calcd. For $C_{28}H_{27}NO_5$ (457.19): C, 73.51; H, 5.95; N, 3.06. Found: C, 73.62; H, 5.96; N, 3.14.

3.1.2.4: (E)-1-Benzyl-3-(2-hydroxybenzylidene)-5-(4-methoxyphenyl)-1H-pyrrol-2-(3H)-one 4d.

Orange red crystals; (method A; 0.75 g, 65.5% yield, method B; 0.64 g, 55.5% yield); mp = 222-224°C; IR (KBr) ν_{\max} = 1680 cm^{-1} (C=O of pyrrolone); 1H -NMR (400 MHz, $CDCl_3$) δ (ppm) = 3.80 (s, 3H, OCH_3), 4.88 (s, 2H, N- CH_2), 6.21 (s, 1H, olefinic H), 6.84 (d, 2H, J = 7.6 Hz, ArH), 6.87-6.90 (m, 2H, Ar), 6.93 (s, 1H, OH), 7.01 (d, 2H, J = 7.6 Hz, ArH), 7.18-7.21 (m, 3H, ArH), 7.22-7.27 (m, 3H, ArH), 7.65 (d, 1H, ArH, J = 7.6 Hz), 8.33 (s, 1H, pyrrolone ring); ^{13}C NMR (75 MHz, $DMSO-d_6$) δ (ppm) = 160.1, 160.1, 157.3, 148.1, 138.0, 131.3, 129.6, 129.1, 128.5, 127.8, 126.9, 126.3, 126.1, 123.1, 122.4, 119.7, 115.9, 114.2, 99.8, 55.3, 43.8. Anal. Calcd. For $C_{25}H_{21}NO_3$ (383.15): C, 78.31; H, 5.52; N, 3.65. Found: C, 78.49; H, 5.61; N, 3.73.

Crystal and molecular structure of 4d ($C_{25}H_{21}NO_3$)

The study of the **4d** was undertaken to establish its three dimensional structure. All diagrams and calculations were performed using maXus³⁴ (Bruker Nonius, Delft and MacScience, Japan). Atomic scattering factors from Waasmaier and Kirfel.³⁵ Data collection: KappaCCD. Cell refinement: HKL Scalepack (Otwinowski and Minor).³⁶ Data reduction: Denzo and Scalepak (Otwinowski & Minor).³⁶ Programs used to solve structure: SIR92 (Altomare *et al.*).³⁷ Programs used to refine structure: maXus (Mackay *et al.*).³¹ Molecular graphics: ORTEP (Johnson).³⁸ Software used to prepare material for publication: maXus (Mackay *et al.*).³⁴ The X-ray study of the pyrrolone **4d** revealed that, the pyrrolone **4d** present in (*E*) configuration.

3.1.2.5: (E)-1-Benzyl-3-(4-hydroxy-3-methoxybenzylidene)-5-(4-methoxyphenyl)-1H-pyrrol-2(3H)-one 4e.

Red crystals; (method A; 0.67 g, 56.2% yield, method B; 0.79 g, 64.0% yield); mp = 176-177°C; IR (KBr) ν_{\max} = 1686 cm^{-1} (C=O of pyrrolone); $^1\text{H-NMR}$ (400 MHz, CDCl_3) δ (ppm) = 3.81 (s, 3H, OCH_3), 3.91 (s, 3H, OCH_3), 4.83 (s, 2H, N- CH_2), 6.17 (s, 1H, olefinic H), 6.87 (d, 2H, J = 6.8 Hz, ArH), 6.96 (d, 1H, J = 8.4 Hz, ArH), 7.09 (d, 2H, J = 6.8 Hz, ArH), 7.13-7.14 (m, 1H, ArH), 7.19-7.24 (m, 3H, ArH), 7.26-7.29 (m, 4H; 3H, ArH and OH) 7.43 (s, 1H, H-4 pyrrolone ring); $^{13}\text{C NMR}$ (75 MHz, CDCl_3) δ (ppm) = 160.1, 147.5, 147.4, 146.7, 138.0, 132.6, 129.6, 129.4, 128.5, 128.4, 127.5, 127.0, 124.7, 124.6, 123.9, 115.0, 114.1, 112.5, 99.9, 56.0, 55.3, 44.6. Anal. Calcd. $\text{C}_{26}\text{H}_{23}\text{NO}_4$ (413.16): C, 75.53; H, 5.61; N, 3.39. Found: C, 75.65; H, 5.68; N, 3.44.

3.1.2.6: (E)-1-Benzyl-3-(4-chlorobenzylidene)-5-(4-methoxyphenyl)-1H-pyrrol-2(3H)-one 4f.

Red crystals; (method A; 0.75 g, 62.6% yield, method B; 0.91 g, 75.3% yield); mp = 113-115°C; IR (KBr) ν_{\max} = 1691 cm^{-1} (C=O of pyrrolone); $^1\text{H-NMR}$ (400 MHz, CDCl_3) δ (ppm) = 3.82 (s, 3H, OCH_3), 4.84 (s, 2H, N- CH_2), 6.14 (s, 1H, olefinic H), 6.87 (d, 2H, J = 8.8 Hz, ArH), 7.08 (d, 2H, J = 8.0 Hz, ArH), 7.19-7.26 (m, 5H, ArH), 7.36 (d, 2H, J = 8.0 Hz, ArH), 7.40 (s, 1H, H-4 pyrrolone ring), 7.56 (d, 2H, J = 8.8 Hz, ArH); EI-MS (70 eV) m/z (%) 401 (M^+ , 72), 369 (4), 310 (5), 308 (24), 294 (4), 260 (5), 275 (45), 232 (20), 203 (17), 184 (7), 135 (10), 134 (10), 108 (1), 107 (7), 95 (10), 91 (100), 83 (4), 77 (13), 65 (18). Anal. Calcd. $\text{C}_{25}\text{H}_{20}\text{ClNO}_2$ (401.12): C, 74.71; H, 5.02; N, 3.49. Found: C, 74.84; H, 5.08; N, 3.61.

3.1.3: General procedure for preparation of substituted-2-benzylidene-4-(4-methoxyphenyl)-4-oxobutanehydrazide 5a-f.

To a solution of the appropriate furanone (0.003 mol) in absolute ethanol, hydrazine monohydrate (0.006 mol) was added. The reaction mixture was left for 1 day at room temperature. The solid mass that was formed was filtered off and recrystallized with absolute ethanol afforded compounds **5a-f**.

3.1.3.1: 2-Benzylidene-4-(4-methoxy phenyl)-4-oxobutanehydrazide 5a.

White powder; (0.42 g, 45.2% yield); mp = 144-145°C [reported³⁹ 176°C]; IR (KBr) ν_{\max} = broad band 3200-3267 cm^{-1} (NHNH_2), 1678 cm^{-1} (C=O benzoyl), 1656 cm^{-1} (C=O

hydrazide); $^1\text{H-NMR}$ (400 MHz, $\text{DMSO-}d_6$) δ (ppm) = 3.12 (d, 1H, $^2J = 17.6$ Hz, COCH_2), 3.21 (d, 1H, $^2J = 17.6$ Hz, COCH_2), 3.75 (s, 3H, OCH_3), 4.39 (s, 2H, NH_2), 6.58 (s, H, olefinic H), 6.90 (d, 2H, $J = 8.4$ Hz, ArH), 7.28 (d, 2H, $J = 8.4$ Hz, ArH), 7.30-7.36 (m, 1H, ArH), 7.38(s, H, NH), 7.42 (d, 2H, $J = 7.2$ Hz, ArH), 7.50 (d, 2H, $J = 7.2$ Hz, ArH).

3.1.3.2: 2-(4-Methoxybenzylidene)-4-(4-methoxyphenyl)-4-oxobutanehydrazide 5b.

White powder; (0.57 gm, 55.9% yield); mp = 138-140°C; IR (KBr) ν_{max} = broad band 3200-3319 cm^{-1} (NHNH_2), 1682 cm^{-1} (C=O benzoyl), 1650 cm^{-1} (C=O hydrazide); $^1\text{H-NMR}$ (400 MHz, CDCl_3) δ (ppm) = 3.35 (d, 1H, $^2J = 17.6$ Hz, COCH_2), 3.61 (d, 1H, $^2J = 17.6$ Hz, COCH_2), 3.79 (s, 3H, OCH_3), 3.80 (s, 3H, OCH_3), 3.98 (s, 2H, NH_2), 6.80 (d, 2H, $J = 8.8$ Hz, ArH), 6.88 (d, 2H, $J = 8.8$ Hz, ArH), 7.27 (m, 3H; 1H, ArH and 1H, olefinic H), 7.34-7.37 (m, 3H; 2H, ArH and NH). Anal. Calcd. For $\text{C}_{19}\text{H}_{20}\text{N}_2\text{O}_4$ (340.14): C, 67.05; H, 5.92; N, 8.23. Found: C, 67.39; H, 5.95; N, 8.40.

3.1.3.3: 4-(4-Methoxyphenyl)-4-oxo-2-(3,4,5-trimethoxybenzylidene)butanehydrzide 5c.

White powder; (0.48 g, 40.0% yield); mp = 93-95°C; IR (KBr) ν_{max} = broad band 3200-3318 cm^{-1} (NHNH_2), 1679 cm^{-1} (C=O benzoyl), 1654 cm^{-1} (C=O hydrazide); $^1\text{H-NMR}$ (400 MHz, $\text{DMSO-}d_6$) δ (ppm) = 3.12 (d, 1H, $^2J = 17.2$ Hz, COCH_2), 3.21 (d, 1H, $^2J = 17.2$ Hz, COCH_2), 3.67 (s, 3H, OCH_3), 3.75 (s, 3H, OCH_3), 3.79 (s, 6H, 2OCH_3), 4.36 (s, 2H, NH_2), 6.57 (s, H, olefinic H), 6.80 (s, 2H, ArH), 6.91 (d, 2H, $J = 8.7$ Hz, ArH), 7.25 (s, 1H, NH), 7.28 (d, 2H, $J = 8.7$ Hz, ArH); EI-MS (70 eV) m/z (%) 400 (M^+ , 57), 308 (24), 275 (45), 232 (20), 203 (17), 135 (10), 91 (100), 77 (13). Anal. Calcd. For $\text{C}_{21}\text{H}_{24}\text{N}_2\text{O}_6$ (400.16): C, 62.99; H, 6.04; N, 7.00. Found: C, 63.08; H, 6.09; N, 7.13.

3.5.4. 2-(2-Hydroxybenzylidene)-4-(4-methoxyphenyl)-4-oxobutanehydrazide 5d.

Buff powder; (0.39 g, 40.0% yield); mp = 129-130°C; IR (KBr) ν_{max} = Broad band 3200-3317 cm^{-1} (NHNH_2 and OH), 1681 cm^{-1} (C=O benzoyl), 1650 cm^{-1} (C=O hydrazide); $^1\text{H-NMR}$ (400 MHz, $\text{DMSO-}d_6$) δ (ppm) = 3.07 (d, 1H, $^2J = 16.0$ Hz, COCH_2), 3.18 (d, 1H, $^2J = 16.0$ Hz, COCH_2), 3.77 (s, 3H, OCH_3), 4.34 (s, 2H, NH_2), 6.54 (s, H, olefinic H), 6.90-6.92 (m, 2H, ArH), 6.95-6.97 (m, 3H; 2H, ArH and OH), 7.23 (s, 1H, NH), 7.27 (d, 2H, $J = 8.0$ Hz, ArH), 7.45 (d, 2H, $J = 8.0$ Hz, ArH). Anal. Calcd. For $\text{C}_{18}\text{H}_{18}\text{N}_2\text{O}_4$ (326.13): C, 66.25; H, 5.56; N, 8.58. Found: C, 66.39; H, 5.63; N, 8.74.

3.5.5. 2-(4-Hydroxy-3-methoxybenzylidene)-4-(4-methoxyphenyl)-4-oxobutane-hydrazide 5e.

Pale yellow powder; (0.45 g, 42.0% yield); mp = 120-122°C; IR (KBr) ν_{\max} = broad band 3200-3276 cm^{-1} (NHNH₂ and OH), 1671 cm^{-1} (C=O benzoyl), 1647 cm^{-1} (C=O hydrazide); ¹H-NMR (400 MHz, CDCl₃) δ (ppm) = 3.17 (d, 1H, ²J = 17.6 Hz, COCH₂), 3.32 (d, 1H, ²J = 17.6 Hz, COCH₂), 3.79 (s, 3H, OCH₃), 3.83 (s, 5H, OCH₃ and NH₂), 6.83 (s, H, olefinic H), 6.85-6.95 (m, 4H, ArH), 7.27 (s, 2H, OH and NH), 7.34-7.36 (m, 3H, ArH); EI-MS (70 eV) *m/z* (%) 457 (M⁺, 69), 292 (83), 201 (75), 135 (10), 110 (100), 78 (78). Anal. Calcd. For C₁₉H₂₀N₂O₅ (356.14): C, 64.04; H, 5.66; N, 7.86. Found: C, 64.17; H, 5.72; N, 7.94.

3.5.6. 2-(4-Chlorobenzylidene)-4-(4-methoxyphenyl)-4-oxobutanehydrazide 5f.

White powder; (0.44 g, 42.80% yield); mp = 99-101°C; IR (KBr) ν_{\max} = broad band 3200-3311 cm^{-1} (NHNH₂), 1681 cm^{-1} (C=O benzoyl), 1654 cm^{-1} (C=O hydrazide); ¹H-NMR (400 MHz, CDCl₃) δ (ppm) = 3.17 (d, 1H, ²J = 18.0 Hz, COCH₂), 3.32 (d, 1H, ²J = 18.0 Hz, COCH₂), 3.84 (s, 3H, OCH₃), 3.95 (s, 2H, NH₂), 6.68 (m, 2H; 1H, ArH and olefinic H), 7.05 (d, 1H, J = 8.4 Hz, ArH), 7.19-7.35 (m, 5H; 4H, ArH and 1H, NH), 7.37-7.51 (m, 1H, ArH), 7.70 (d, 1H, J = 8.4 Hz, ArH); EI-MS (70 eV) *m/z* (%) 344 (M⁺, 1), 327 (100), 311 (34), 297 (10), 233 (20), 203 (27), 135 (77), 92 (15), 76 (37). Anal. Calcd. For C₁₈H₁₇ClN₂O₃ (344.09): C, 62.70; H, 4.97; N, 8.12. Found: C, 62.83; H, 5.01; N, 8.25.

3.6. General procedure for synthesis of substituted 3-benzylidene-1-

((benzylidene)amino)-5-(4-methoxyphenyl)-1H-pyrrol-2(3H)-one (6a, 6f & 6g-j).

Preparation of 6a, 6f: - Heating at reflux a mixture of the appropriate hydrazide **5a** or **5f** (0.001 mol) and *p*-methoxybenzaldehyde (0.001 mol) in ethanol for 13-24 h. The solvent was evaporated under reduced pressure and the obtained residue was crystallized from ethanol affording compound **6a** or **6f**.

Preparation of 6g-j: - A mixture of the hydrazide **5f** (0.001 mol) and different aromatic aldehyde (0.001 mol) in ethanol was left in room temperature for 2 days. The obtained precipitate was filtered off and washed to give compounds **6g-j**.

3.6.1. 3-(4-Methoxybenzylidene)-1-((4-methoxybenzylidene)amino)-5-(4-methoxyphenyl)-1H-pyrrol-2(3H)-one 6a.

Orange powder; (0.23 g, 13 h, 51.7% yield); mp = 191-193°C; IR (KBr) ν_{\max} = 1691 cm^{-1} (C=O of pyrrolone); $^1\text{H-NMR}$ (400 MHz, CDCl_3) δ (ppm) = 3.82 (s, 3H, OCH_3), 3.83 (s, 3H, OCH_3), 3.85 (s, 3H, OCH_3), 6.33 (s, 1H, olefinic H), 6.84 (d, 2H, J = 8.8 Hz, ArH), 6.93-6.96 (m, 4H, ArH), 7.37 (s, 1H, H-4 pyrrolone ring), 7.62 (d, 2H, J = 5.2 Hz, ArH), 7.64 (d, 2H, J = 5.2 Hz, ArH), 7.66 (d, 2H, J = 8.8 Hz, ArH), 9.57 (s, 1H, $\text{CH}=\text{N}$); ^{13}C NMR (75 MHz, CDCl_3) δ (ppm) = 161.8, 161.0, 159.6, 159.5, 152.8, 147.2, 132.3, 129.8, 128.2, 127.8, 126.2, 122.6, 114.1, 113.9, 113.0, 103.3, 103.0, 98.3, 55.2, 55.1; EI-MS (70 eV) m/z (%): 440 (M^+ , 60), 379 (12), 322 (13), 308 (14), 307 (13), 286 (13), 248 (18), 186 (13), 171 (19), 141 (17), 144 (16), 135 (22), 133 (16), 121 (21), 120 (14), 108 (21), 94 (13), 80 (100), 79 (25), 77 (15), 64 (56), 55 (64). Anal. Calcd. For $\text{C}_{27}\text{H}_{24}\text{N}_2\text{O}_4$ (440.17): C, 73.62; H, 5.49; N, 6.36. Found: C, 73.70; H, 5.51; N, 6.45.

3.6.2. 3-(4-Chlorobenzylidene)-1-((4-methoxybenzylidene)amino)-5-(4-methoxyphenyl)-1H-pyrrol-2(3H)-one 6f.

Orange crystal; (0.23 g, 24 h, 51.7% yield); mp = 184-186°C; IR (KBr) ν_{\max} = 1694 cm^{-1} (C=O of pyrrolone); $^1\text{H-NMR}$ (300 MHz, CDCl_3) δ (ppm) = 3.86 (s, 3H, OCH_3), 3.89 (s, 3H, OCH_3), 6.30 (s, 1H, olefinic H), 6.91 (d, 2H, J = 8.7 Hz, ArH), 6.96 (d, 2H, J = 9.0 Hz, ArH), 7.36 (s, 1H, H-4 pyrrolone ring), 7.40 (d, 2H, J = 8.4 Hz, ArH), 7.58 (d, 2H, J = 8.4 Hz, ArH), 7.66 (d, 2H, J = 8.7 Hz, ArH), 7.69 (d, 2H, J = 9.0 Hz, ArH), 9.56 (s, 1H, $\text{CH}=\text{N}$); EI-MS (70 eV) m/z (%): 446 ($\text{M}+2$, 100), 311 (93), 296 (16), 268 (17), 247 (4), 205 (6), 189 (16), 148 (10), 134 (35), 107 (5), 79 (2), 91 (20), 77 (18), 64 (13). Anal. Calcd. For $\text{C}_{26}\text{H}_{21}\text{ClN}_2\text{O}_3$ (444.12): C, 70.19; H, 4.76; N, 6.30. Found: C, 70.34; H, 4.82; N, 6.43.

3.6.3. 1-(Benzylideneamino)-3-(4-chlorobenzylidene)-5-(4-methoxyphenyl)-1H-pyrrol-2(3H)-one 6g.

Orange crystal; (0.16 g, 39.0% yield); mp = 146-148°C; IR (KBr) ν_{\max} = 1697 cm^{-1} (C=O of pyrrolone); $^1\text{H-NMR}$ (400 MHz, CDCl_3) δ (ppm) = 3.90 (s, 3H, OCH_3), 6.33 (s, 1H, olefinic H), 6.99 (d, 2H, J = 8.0 Hz, ArH), 7.28 (s, 1H, H-4 pyrrolone ring), 7.39-7.44 (m, 5H, ArH), 7.61 (d, 2H, J = 8.0 Hz, ArH), 7.72 (d, 4H, J = 7.2 Hz, ArH), 9.70 (s, 1H,

$CH=N$). Anal. Calcd. For $C_{25}H_{19}ClN_2O_2$ (414.11): C, 72.37; H, 4.62; N, 6.75. Found: C, 72.45; H, 4.65; N, 6.83.

3.6.4. 3-(4-Chlorobenzylidene)-1-((3,4-dimethoxybenzylidene)amino)-5-(4-methoxyphenyl)-1H-pyrrol-2(3H)-one 6h.

Red crystal; (0.25 g, 51.7% yield); mp = 176-178°C; IR (KBr) ν_{max} = 1702 cm^{-1} (C=O of pyrrolone); 1H -NMR (400 MHz, $CDCl_3$) δ (ppm) = 3.89 (s, 3H, OCH_3), 3.92 (s, 3H, OCH_3), 3.95 (s, 3H, OCH_3), 6.33 (s, 1H, olefinic H), 6.90 (d, 1H, J = 8.4 Hz, ArH), 6.97 (d, 2H, J = 8.4 Hz, ArH), 7.29 (s, 1H, H-4 pyrrolone ring), 7.36 (d, 2H, J = 8.8 Hz, ArH), 7.43 (d, 2H, J = 8.4 Hz, ArH), 7.61 (d, 2H, J = 8.4 Hz, ArH), 7.73 (d, 2H, J = 8.8 Hz, ArH), 9.58 (s, 1H, $CH=N$). Anal. Calcd. For $C_{27}H_{23}ClN_2O_4$ (474.13): C, 68.28; H, 4.88; N, 5.90. Found: C, 68.39; H, 4.86; N, 6.04.

3.6.5. 3-(4-Chlorobenzylidene)-5-(4-methoxyphenyl)-1-((3,4,5-trimethoxybenzylidene)amino)-1H-pyrrol-2(3H)-one 6i.

Red needle crystals; (0.26 g, 52.0% yield); mp = 196-198°C; IR (KBr) ν_{max} = 1707 cm^{-1} (C=O of pyrrolone); 1H -NMR (400 MHz, $CDCl_3$) δ (ppm) = 3.89 (s, 6H, $2OCH_3$), 3.91 (s, 3H, OCH_3), 3.98 (s, 3H, OCH_3), 6.35 (s, 1H, olefinic H), 6.97-6.99 (m, 2H, ArH), 7.28 (s, 2H, ArH), 7.39 (s, 1H, H-4 pyrrolone ring), 7.43 (d, 2H, J = 8.0 Hz, ArH), 7.62 (d, 2H, J = 8.0 Hz, ArH), 7.73 (d, 2H, J = 8.4 Hz, ArH), 9.61 (s, 1H, $CH=N$). Anal. Calcd. For $C_{28}H_{25}ClN_2O_5$ (504.15): C, 66.60; H, 4.99; N, 5.55. Found: C, 66.75; H, 5.03; N, 5.67.

3.6.6. 3-(4-Chlorobenzylidene)-1-((4-chlorobenzylidene)amino)-5-(4-methoxyphenyl)-1H-pyrrol-2(3H)-one 6j.

Red crystals; (0.25 gm, 55.0 % yield); mp = 211-212°C; IR (KBr) ν_{max} = 1697 cm^{-1} (C=O of pyrrolone); 1H -NMR (400 MHz, $CDCl_3$) δ (ppm) = 3.91 (s, 3H, OCH_3), 6.34 (s, 1H, olefinic H), 6.99 (d, 2H, J = 7.2 Hz, ArH), 7.39 (s, 1H, pyrrolone ring), 7.43-7.49 (m, 4H, ArH), 7.61-7.63 (m, 2H, ArH), 7.64 (d, 2H, J = 8.0 Hz, ArH), 7.68 (d, 2H, J = 8.0 Hz, ArH), 9.70 (s, 1H, $CH=N$). Anal. Calcd. For $C_{25}H_{18}Cl_2N_2O_2$ (448.07): C, 66.83; H, 4.04; N, 6.23. Found: C, 66.98; H, 4.11; N, 6.37.

3.7. General procedure for preparation of substituted 4-(benzyl)-6-(4-methoxyphenyl)pyridazin-3(2H)-one 7a-f.

Method A: - Heating at reflux of the appropriate hydrazide **5** (0.001 mol) in 6 M hydrochloric acid (20 mL) for 1 h, the reaction mixture was cooled, filtered off, and recrystallized afforded the corresponding pyridazinone **7a-f**.

Method B: - Heating at reflux a mixture of the appropriate furanone **2** (0.001 mol) and hydrazinemonohydrate (100%, 0.002 mol) in ethanol for 4-24 h, the solvent was evaporated under reduced pressure. The obtained residue was recrystallized from ethanol afforded compounds **7a-f**.

3.7.1. 4-(Benzyl)-6-(4-methoxyphenyl)pyridazin-3(2H)-one 7a.

Buff powder; (method A; 0.19 g, 65.0% yield, method B; 10 h, 0.21 g, 70.6% yield); mp = 191-193°C; IR (KBr) ν_{\max} = 1648 cm^{-1} (C=O of pyridazinone); $^1\text{H-NMR}$ (400 MHz, CDCl_3) δ (ppm) = 3.84 (s, 3H, OCH_3), 4.12 (s, 2H, CH_2), 6.85 (d, 2H, J = 8.8 Hz, ArH), 7.23-7.24 (m, 2H, ArH), 7.27-7.29 (m, 2H; 1H, ArH and 1H, H-5 pyridazinone ring), 7.33-7.37 (m, 2H, ArH), 7.58 (d, 2H, J = 8.8 Hz, ArH), 11.97 (s, 1H, NH). Anal. Calcd. For $\text{C}_{18}\text{H}_{16}\text{N}_2\text{O}_2$ (292.12): C, 73.95; H, 5.52; N, 9.58. Found: C, 74.03; H, 5.59; N, 9.67.

3.7.2. 4-(4-Methoxybenzyl)-6-(4-methoxyphenyl)pyridazin-3(2H)-one 7b.

White crystals, (method A; 0.19 g, 60.0% yield, method B; 6 h, 0.24 g, 75.1% yield); mp = 201-203°C; IR (KBr) ν_{\max} = 1650 cm^{-1} (C=O of pyridazinone); $^1\text{H-NMR}$ (400 MHz, CDCl_3) δ (ppm) = 3.82 (s, 3H, OCH_3), 3.83 (s, 3H, OCH_3), 3.94 (s, 2H, CH_2), 6.90-6.94 (m, 4H, ArH), 7.21 (d, 2H, J = 8.4 Hz, ArH), 7.26 (s, 1H, H-5 pyridazinone ring), 7.61 (d, 2H, J = 8.4 Hz, ArH), 12.09 (s, 1H, NH); $^{13}\text{C NMR}$ (75 MHz, DMSO-d_6) δ (ppm) = 160.7, 160.2, 160.2, 158.0, 143.9, 143.2, 130.2, 127.7, 127.4, 127.1, 114.4, 114.0, 55.4, 55.1, 34.4; EI-MS (70 eV) m/z (%): 323 (M^+ , 100), 307 (43), 290 (1), 249 (4), 189 (9), 186 (1), 171 (2), 150 (6), 146 (35), 134 (11), 132 (22), 110 (4), 108 (7), 106 (2), 95 (1), 94 (2), 92 (10), 80 (2), 77 (22). Anal. Calcd. For $\text{C}_{19}\text{H}_{18}\text{N}_2\text{O}_3$ (322.13): C, 70.79; H, 5.63; N, 8.69. Found: C, 70.92; H, 5.67; N, 8.84.

3.7.3. 6-(4-Methoxyphenyl)-4-(3,4,5-trimethoxybenzyl)pyridazin-3(2H)-one 7c.

White needle crystals; (method A; 0.27 g, 70.0% yield, method B; 5 h, 0.30 g, 78.7% yield); mp = 199-201°C; IR (KBr) ν_{\max} = 1655 cm^{-1} (C=O of pyridazinone); $^1\text{H-NMR}$

(300 MHz, DMSO- d_6) δ (ppm) = 3.63 (s, 2H, CH₂), 3.74 (s, 3H, OCH₃), 3.78 (s, 3H, OCH₃), 3.80 (s, 6H, 2OCH₃), 6.68 (s, 2H, ArH), 7.11 (d, 2H, J = 9.0 Hz, ArH), 7.20 (d, 2H, J = 9.0 Hz, ArH), 7.78 (s, 1H, H-5 pyridazinone ring), 13.00 (s, 1H, NH); ¹³C NMR (75 MHz, DMSO- d_6) δ (ppm) = 160.5, 160.1, 159.9, 159.8, 152.7, 143.7, 142.4, 136.1, 133.7, 127.6, 127.3, 126.9, 114.2, 106.4, 59.8, 55.8, 55.1, 35.2; EI-MS (70 eV) m/z (%): 382 (M⁺, 60), 368 (12), 367 (56), 351 (58), 275 (13), 244 (72), 215 (2), 188 (5), 186 (100), 171 (2), 167 (4), 149 (4), 144 (84), 137 (6), 135 (2), 131 (94), 109 (8), 107 (5), 106 (55), 95 (12), 94 (2), 80 (12), 78 (69). Anal. Calcd. For C₂₁H₂₂N₂O₅ (382.15): C, 65.96; H, 5.80; N, 7.33. Found: C, 66.28; H, 6.11; N, 7.51.

3.7.4. 4-(2-Hydroxybenzyl)-6-(4-methoxyphenyl)pyridazin-3(2H)-one 7d

Pale brown crystals; (method A; 0.15 g, 50.0% yield, method B; 4 h, 0.26 g, 83.5% yield); mp = 211-212°C; IR (KBr) ν_{\max} = 1644 cm⁻¹ (C=O of pyridazinone); ¹H-NMR (300 MHz, DMSO- d_6) δ (ppm) = 3.78 (s, 2H, CH₂), 3.79 (s, 3H, OCH₃), 6.74-6.79 (m, 1H, ArH), 6.82 (d, 1H, J = 7.5 Hz, ArH), 7.00 (d, 2H, J = 8.7 Hz, ArH), 7.07-7.12 (m, 1H, ArH), 7.15 (d, 1H, J = 7.5 Hz, ArH), 7.58 (s, 1H, H-5 pyridazinone ring), 7.61 (d, 2H, J = 8.7 Hz, ArH), 9.58 (s, 1H, OH), 13.11 (s, 1H, NH); ¹³C NMR (75 MHz, DMSO- d_6) δ (ppm) = 161.2, 161.0, 160.0, 155.2, 144.0, 142.2, 130.6, 127.6, 127.3, 127.3, 126.8, 123.8, 119.1, 115.5, 114.2, 56.1, 30.6. Anal. Calcd. For C₁₈H₁₆N₂O₃ (308.12): C, 70.12; H, 5.23; N, 9.09. Found: C, 70.20; H, 5.27; N, 9.22.

3.7.5. 4-(4-Hydroxy-3-methoxybenzyl)-6-(4-methoxyphenyl)pyridazin-3(2H)-one 7e

White crystals; (method A; 0.20 g, 60.0% yield, method B; 5 h, 0.25 g, 73.5% yield); mp = 224-226°C; IR (KBr) ν_{\max} = 1652 cm⁻¹ (C=O of pyridazinone); ¹H-NMR (400 MHz, CDCl₃) δ (ppm) = 3.78 (s, 3H, OCH₃), 3.83 (s, 3H, OCH₃), 3.87 (s, 2H, CH₂), 6.73 (d, 2H, J = 8.8 Hz, ArH), 6.79 (s, 1H, OH), 6.86-6.90 (m, 2H, ArH), 7.22 (s, 1H, ArH), 7.24 (s, 1H, H-5 pyridazinone ring), 7.57 (d, 2H, J = 8.8 Hz, ArH), 11.98 (s, 1H, NH); EI-MS (70 eV) m/z (%): 338 (M⁺, 100), 324 (7), 323 (22), 308 (3), 307 (6), 231 (2), 216 (20), 201 (4), 188 (4), 187 (7), 171 (5), 165 (9), 147 (12), 137 (13), 123 (9), 115 (3), 107 (9), 106 (4), 95 (10), 94 (15), 80 (50), 78 (11). Anal. Calcd. For C₁₉H₁₈N₂O₄ (338.13): C, 67.44; H, 5.36; N, 8.28. Found: C, 67.39; H, 5.39; N, 8.42.

3.7.6. 4-(4-Chlorobenzyl)-6-(4-methoxyphenyl)pyridazin-3(2H)-one 7f.

White crystals; (method A; 0.25 g, 75.0% yield, method B; 24 h, 0.26 g, 80.7% yield); mp = 230-232°C; IR (KBr) ν_{\max} = 1661 cm^{-1} (C=O of pyridazinone); $^1\text{H-NMR}$ (400 MHz, CDCl_3) δ (ppm) = 3.82 (s, 3H, OCH_3), 3.93 (s, 2H, CH_2), 6.91 (d, 2H, J = 8.4 Hz, ArH), 7.21-7.26 (m, 3H; 2H, ArH and 1H, H-5 pyridazinone ring), 7.30 (d, 2H, J = 8.4 Hz, ArH), 7.59 (d, 2H, J = 8.0 Hz, ArH), 11.37 (s, 1H, NH); EI-MS (70 eV) m/z (%): 326.24 (M^+ , 100), 291 (7), 189 (21), 150 (32), 115 (86), 89 (62), 63 (45). Anal. Calcd. For $\text{C}_{18}\text{H}_{15}\text{ClN}_2\text{O}_2$ (326.08): C, 66.16; H, 4.63; N, 8.57. Found: C, 66.32; H, 4.39; N, 8.65.

4. Biology

4.1. Cell Culture

Human hepatocarcinoma (HepG2) and breast adenocarcinoma (MCF-7) purchased from ATCC, USA, were used in the cytotoxicity evaluation of the test compounds. Cells were routinely cultured in DMEM (Dulbecco's Modified Eagle's Medium). Media was supplemented with 100 units/mL streptomycin sulfate, 100 units/mL penicillin G sodium, 2 mL-glutamine, 250 ng/mL amphotericin B and 10% fetal bovine serum (FBS). Cells were maintained at 37 °C in humidified air containing 5% CO_2 and harvested by trypsinization. Cells were used when confluence had reached 75%. Samples were dissolved in dimethylsulfoxide (DMSO), and then diluted for the assays. All cell culture material was purchased from Gibco®/Invitrogen, USA. All chemicals were from Sigma/Aldrich, USA, except mentioned. All experiments were repeated three times.

4.2. Cytotoxic activity

Cytotoxicity of tested samples was measured against each cell line using the MTT Cell Viability Assay. MTT (3-[4,5-dimethylthiazole-2-yl]-2,5-diphenyltetrazolium bromide) assay is based on the ability of active mitochondrial dehydrogenase enzyme of living cells to cleave the tetrazolium rings of the yellow MTT and form a dark blue insoluble formazan crystals which is largely impermeable to cell membranes, resulting in its accumulation within healthy cells. Solubilization of the cells results in the liberation of crystals, which are then solubilized. The number of viable cells is directly proportional to the level of soluble formazan dark blue color. The extent of the reduction of MTT was quantified by measuring the absorbance at 570 nm.⁴⁰ Briefly, cells (0.5×10^5 cells/ well), in serum-free media, were plated in a flat bottom 96-well microplate, and treated with 20 μl of serial concentrations of the tested samples for 48 h at 37° C, in a humidified 5%

CO₂ atmosphere. After incubation, media were removed and 40 µl MTT solution (: 5mg/mL of MTT in 0.9%NaCl) in each well were added and Incubated for an additional 4 h. MTT crystals were solubilized by adding 180 µl of acidified isopropanol / well and plate was shaken at room temperature, followed by photometric determination of the absorbance at 570 nm using microplate ELISA reader with using paclitaxel as a reference standard. Triplicate repeats were performed for each concentration and the average was calculated. Data were expressed as the percentage of relative viability compared with the untreated cells compared with the vehicle control, with cytotoxicity indicated by <100% relative viability. Percentage of relative viability was calculated using the following equation: [Absorbance of treated cells/ Absorbance of control cells] X 100. Then the half maximal inhibitory concentration (IC₅₀) was calculated from the equation of the dose response curve.

The total protein content of the lysates of treated and untreated cells was prepared and measured as reported.^{41,42}

On the other hand, the methodology of the NCI anticancer screening has been described in detail elsewhere (<http://www.dtp.nci.nih.gov>.) Briefly, the primary anticancer assay was performed at approximately 60 human tumor cell lines panel derived from nine neoplastic diseases, in accordance with the protocol of the Drug Evaluation Branch, National Cancer Institute, Bethesda. Tested compounds were added to the culture at a single concentration (10⁻⁵ M) and the cultures were incubated for 48 h. End point determinations were made with a protein binding dye, SRB. Results for each tested compound were reported as the percent of growth of the treated cells when compared to the untreated control cells. The percentage growth was evaluated spectrophotometrically Versus controls not treated with test agents.

4.3. Tubulin polymerization inhibition

Tubulin level was determined in cell lysates by ELISA according to the method originally developed by Kawahira *et al*⁴³ and Noel *et al*⁴⁴ with some modifications as reported by us⁴², immunohistochemical detection of tubulin in fixed cells were done.

Reagents preparation: 0.1M Citrate buffer pH to 6.0: 9 mL of 0.1M citric acid solution was added to 41 mL of 1M sodium citrate solution and the volume was adjusted to 500mL by deionized water. Antigen retrieval solution: 50mL of 0.1M citrate buffer, 500 mL of Triton-100, and 250 mL of Tween-20 were mixed together and the final volume was adjusted to 500mL by deionized water. Blocking solution: 50mL of 0.1M citrate

buffer, 500 mL of Triton 100, 250 mL of Tween-20, and 25mL of FBS were mixed together and the final volume was adjusted to 500mL by deionized water.

Procedure: Slides of fixed cells were rinsed in three changes of PBS. Antigen retrieval step, by which the availability of the antigen for interaction with a specific antibody is maximized, was performed by immersing slides in antigen retrieval solution and incubated in a water bath at 95–99°C for 20 min. Afterwards, slides were directly transferred to pre-cooled antigen retrieval solution placed at -4°C for 5 min. Non-specific binding of the antibody is prevented by incubating the slides in blocking solution at 37°C for 30 min. Slides were then incubated for 30 min at 37°C with rabbit anti-human tubulin antibody (1:500) diluted with blocking solution. Excess antiserum was rinsed from the slide by immersing in cold buffer for two changes of 5–10 min each. Slides were then incubated at 37°C with goat FITC-anti rabbit IgG (1:2500) diluted with blocking solution. The slides were rinsed in the enzyme substrate till the color developed. Images were visualized using a ApoTime fluorescence microscope (Axiostar Plus, Zeiss, Goettingen, Germany) equipped with image analyzer and digital camera (PowerShot A20, Canon, USA).

4.4. Cell cycle analysis

HepG2 cells (5×10^5) after collection were being treated with the test compound (E)4b, mixed with 4 mL of ice-cold 70% ethanol after washing twice with PBS and re-suspension in 250 μ L of PBS. The cells were centrifuged and the pellets were re-suspended in 1 mL of propidium iodide (PI)/Triton X-100 staining solution (0.1 % Triton X-100 in PBS, 0.2 mg/mL RNase A and 10 μ g/mL PI) and incubated for 30 min at room temperature. The stained cells were analyzed by flow cytometry.

4.5. Docking study

Docking simulation study is performed by Medicinal Chemistry Department Faculty of Pharmacy Assiut University, Assiut, Egypt using Molecular Operating Environment (MOE®) version 2014.09, Chemical Computing Group Inc., Montreal, Canada. The computational software operated under “Windows XP” installed on an Intel Pentium IV PC with a 1.6 GHz processor and 512 MB memory.

The target compounds were constructed into a 3D model using the builder interface of the MOE program. After checking their structures and the formal charges on atoms by 2D depiction, the following steps were carried out:

- All conformers were subjected to energy minimization, all the minimizations were performed with MOE until a RMSD gradient of 0.01 Kcal/mole and RMS (Root Mean Square) distance of 0.1 Å with MMFF94X force-field and the partial charges were automatically calculated.
- The obtained database was then saved as Molecular Data Base (MDB) file to be used in the docking calculations.

Optimization of the target:

The X-ray crystallographic structure of the target TUBULIN-COLCHICINE: STATHMIN-LIKE DOMAIN COMPLEX [1SA0] was obtained from Protein data bank. The compounds were docked on the β -subunit of the target.

The enzyme was prepared for docking studies by:

- The co-crystallized ligand, DAMA-colchicine was deleted.
- Hydrogen atoms were added to the system with their standard geometry.
- The atoms connection and type were checked for any errors with automatic correction.
- Selection of the receptor and its atoms potential were fixed.

Docking of the target molecules to TUBULIN active site

Docking of the target compounds was done using MOE-Dock software. The following methodology was generally applied:

- The enzyme active site file was loaded, and the Dock tool was initiated. The program specifications were adjusted to:
 - Dummy atoms as the docking site.
 - Triangle matcher as the placement methodology to be used.
 - London dG as Scoring methodology to be used and was adjusted to its default values.
- The MDB file of the ligand to be docked was loaded and Dock calculations were run automatically.
- The obtained poses were studied and the poses showed best ligand-enzyme interactions were selected and stored for energy calculations.

5. Conclusion

A new pyrrol-2(3*H*)-ones and pyridazin-3 (2*H*)-ones derivatives are synthesized and confirmed with different spectroscopic techniques. The *E* form of pyrrolones **4** have good cytotoxicity activity than the open amide form while the *Z* form has less cytotoxicity activity, also the hydrazides have cytotoxicity activity better than their

corresponding cyclized pyridazinone form if the benzylidene ring have electron donating group. Compounds (**E**)**4b**, **6f** and **7f** exhibited remarkable cytotoxic effect on HepG2, with IC₅₀ of 11.47, 7.11 and 14.8 μM, respectively while compounds (**E**)**4b** and **6f** showed promising activity on MCF-7 with IC₅₀ of 18.58 and 19.49 μM, respectively. Compounds (**E**)**4b**, **6f**, **7d** and **7f** showed a variable inhibitory activity of cellular localization of tubulin. They experienced alteration in cellular morphology with atrophic changes or disappearance of the radial microtubules of resting cells with abnormal distribution pattern of tubulin. Moreover, flow cytometric analysis indicated that HepG2 cells treated with (**E**)**4b** showed a predominated growth arrest at the S-phase higher than that of G2/M-phase (P <0.01) as compared with control cells. Molecular modeling studies indicated that compound (**E**)**4b** was docked into colchicines binding site of tubulin with spontaneous interaction. The binding mode of the cyclized *E*-pyrrolones **4E** is different from its corresponding **Z** and the open chain amides **3**. Also, binding mode of the hydrazides is different from those of the corresponding pyridazin-3(2*H*)-ones. This may be the reason for the difference in biological activity. These results introduce the pyrrolone (**E**)**4b** as new combretastatin-A analogue with restricted rotation of both ring A and ring B with promising anticancer activity.

Acknowledgements

The authors acknowledge the science and technology development fund (STDF) Egypt (project No. 2943 Basic and Applied Research) and faculty of Pharmacy, Minia University for participation in funding this work.

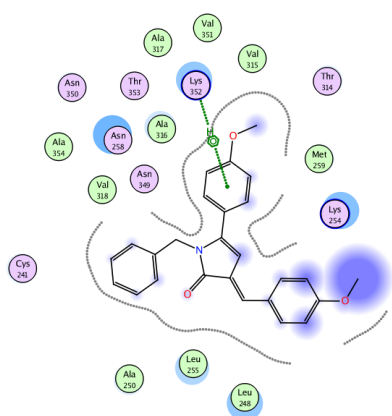
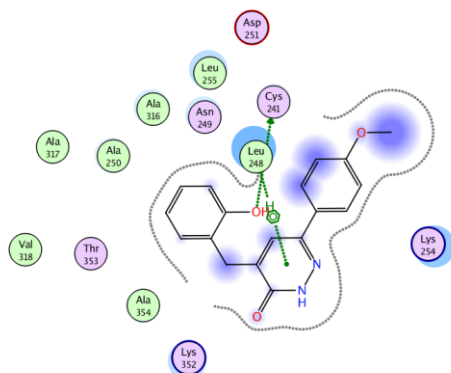
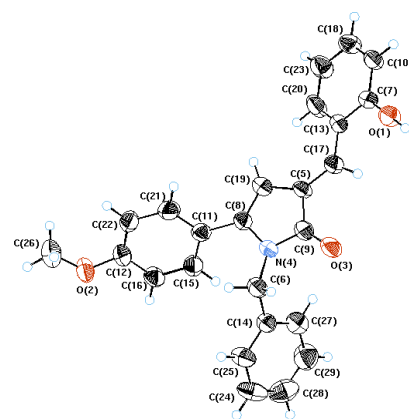
6. References

- 1- K. A. Monk, R. Siles, M. B. Hadimani, B. E. Mugabe, J. F. Ackley, S. W. Studerus, K. Edvardsen, M. L. Trawick, C. M. Garner, M. R. Rhodes, G.R. Pettit, K. G. Pinney, *Bioorganic and Medicinal Chemistry* 14 (2006) 3231-3244.
- 2- F. Bellina, S. Cauteruccio, R. Rossi, *Tetrahedron* 63 (2007) 4571-624.
- 3- Y. Hu, X. Lu, K. Chen, R. Yan, Q.-S. Li, H.-L. Zhu, *Bioorganic and Medicinal Chemistry* 20 (2012) 903-909.
- 4- F. Bellina, S. Cauteruccio, S. Monti, R. Rossia, *Bioorganic & Medicinal Chemistry Letters* 16 (2006) 5757-5762.
- 5- A. B. S. Maya, C. Pérez-Melero, N. Salvador, R. Pelaéz, E. Caballeroa, M. Medardea, *Bioorganic and Medicinal Chemistry* 13 (2005) 2097-2107.

- 6- K. Gaukroger, J. A. Hadfield, N. J. Lawrence, S. Nolan, A. T. MCGOWN, *Organic and Biomolecular Chemistry* 1 (2003) 3033-3037.
- 7- A. I. Hashem, A. S. A. Youssef, K. A. Kandeel, W. S. I. Abou-Elmagd, *European Journal of Medicinal Chemistry* 42 (2007) 934-935.
- 8- A. Husain, M. M. Alam, N. Siddiqui, *Journal of the Serbian Chemical Society* 74 (2009)103-115.
- 9- M. M. Alam, D. P. Sarkar, A. Husain, A. Marella, M. Shaquiquzzaman, M. Akhter, M. S. Yar, O. Alam, F. Azam, *Journal of the Serbian Chemical Society* 26 (2011) 1617-1626.
- 10- A. Husain, M. S. Y. Khan, S. M. Hasan, M. M. Alam, *European Journal of Medicinal Chemistry* 40 (2005) 1394-404.
- 11- D. Chen, Y. Song, Y. Lu, X. Xue, *Bioorganic and Medicinal Chemistry Letters* 23 (2013) 3166-3169.
- 12- S. Olla, F. Manetti, E. Crespan, G. Maga, A. Angelucci, S. Schenone, M. Bologna, M. Botta, *Bioorganic and Medicinal Chemistry Letters* 19 (2009)1512-1516.
- 13- A. Kumar, B. Ahmed, B. Srivastawa, Vaishali, *Der Pharma Chemica*. 4 (2012) 383-391.
- 14- M. M. Alam, A. Husain, S. M. Hasan, Suruchi, T. Anwer, *European Journal of Medicinal Chemistry* 44 (2009) 2636-2642.
- 15- A. Husain, M. M. Alam, S. M. Hasan, M.S. Yar, *Acta Poloniae Pharmaceutica- Drug Research* 66 (2009) 173-180.
- 16- M. Asif, *Chronicles of Young Scientists* 1 (2010) 3-9.
- 17- D. S. Doğruer, M. F. Şahin, E. Küpeli, E. Yeşilada, *Turkish Journal of Chemistry* 27 (2003) 727-738.
- 18- R. Mishra, A. A. Siddiqui, A. Husain, M. Rashid, A. Prakash, M. Tailang, M. Kumar, N. Srivastava, *Journal of the Chilean Chemical Society* 56 (2011) 856-859.
- 19- N. F. Abd El-Ghaffar, M. Kh. Mohamed, M. S. Kadah, A. M. Radwan, G. H. Said, S. N. Abd el Al, *Journal of Chemical and Pharmaceutical Research* 3 (2011) 248-259.
- 20- I. G. Rathish, K. Javed, S. Bano, S. Ahmad, M. S. Alam, K. K. Pillai, *European Journal of Medicinal Chemistry* 44 (2009) 2673-2678.
- 21- K. C. Samanta, M. Asif, Pooja, V. Garg, P. Sharma, R. Singh, *The Electronic Journal of Chemistry* 8 (2011) 245-251.

- 22- M. S. Abdel Halim, A. Radwan, M. A. Saad, G. H. Sayed, M. Khalil, *Journal of the Chemical Society of Pakistan* 15 (1993) 202-206.
- 23- S. Khaidem, S. Sarveswari, R. Gupta, V. Vijaykuma, *International Journal of Research in Pharmacy and Chemistry* 2 (2012) 258-266.
- 24- A. Husain, A. Ahmed, A. Bhandar, V. Ram, *Journal of the Chilean Chemical Society* 56 (2011) 778-780.
- 25- The methodology of the NCI anticancer screening has been described in detail elsewhere (<http://www.dtp.nci.nih.gov>).
- 26- H. Abolhasani, A. Zarghic, M. Hamzeh-Mivehroud, Ali A. Alizadeha, J. S. Mojarrada, S. Dastmalchi, *Iranian Journal of Pharmaceutical Research* 14 (1): (2015) 141-147.
- 27- Y. Jin, P. Qi, Z. Wang, Q. Shen, J. Wang, W. Zhang, H. Song, *Molecules* 16 (2011) 6684-6700.
- 28- N. O. Mahmoodi, M. Jazayri, *Synthetic Communication* 31 (2001) 1467-1475.
- 29- L. S. El-Assal, A. H. Shehab, *Journal of the Chemical Society* (1961) 1658-1662.
- 30- M. S. Y. Khan, A. Husain, S. Sharma, *Indian Journal of Chemistry* 41B (2002) 2160-2171.
- 31- *Indian Journal of Chemistry, B: Organic Chemistry Including Medicinal Chemistry* 26B (1987) 427.
- 32- S. Deo, F. Inam, R. P. Mahashabde, A. N. Jadha, *Asian Journal of Chemistry* 22 (2010) 3362-3368.
- 33- N. F. Eweiss, S. G. Hussain, *Journal of the University of Kuwait, Science* 8 (1981) 185-195.
- 34- S. Mackay, C. J. Gilmore, C. Edwards, N. Stewart, K. Shankland. MaXus computer program for the solution and refinement of crystal structures. Bruker Nonius, The Netherlands, MacScience, Japan and The University of Glasgow. 1999.
- 35- D. Waasmaier, A. Kirfel, *Acta Crystallographica* A51 (1995) 416.
- 36- Z. Otwinowski, W. Minor, *Processing of X-ray Diffraction Data Collected in Oscillation Mode*. In *Methods in Enzymology*. C. W. Carter, R. M. Sweet. New York: Academic Press. 1997, 267, 307.
- 37- A. Altomare, G. Cascarano, C. Giacovazzo, A. Guagliardi, M. C. Burla, G. Polidori, M. Camalli, *Journal of Applied Crystallography* 27 (1994) 435-436.

- 38- C. K. Johnson. A Fortran Thermal-Ellipsoid Plot Program. Report ORNL-5138. *ORTEP--II*. Oak Ridge National Laboratory, Oak Ridge, Tennessee, USA. 1976.
- 39- S. M. Abdel Wahhab, B. M. Awad, S. M. AbdAllah, H. A. Saad, F. A. El Sayed, *Asian Journal of Chemistry* 15 (2003) 865-872.
- 40- M. B. Hansen, S. E. Nielsen, K. Berg, *Journal of Immunology Methods* 119 (1989) 203-210.
- 41- P. K. Smith, R. I. Krohn, G. T. Hermanson, A. K. Mallia, F. H. Gartner, M. D. Provenzano, E. K. Fujimoto, N. M. Goeke, B. J. Olson, D. C. Klenk, *Analytical Biochemistry* 150 (1985) 76-85.
- 42- A. M. Gamal-Eldeen, S. M. El-Daly, I. H. Borai, H. Wafay, A.-R. B. Abdel-Ghaffar, *Photodiagnosis and Photodynamic Therapy* 10 (2013) 446-459.
- 43- K. Kawahira, *Archives of Dermatology Research* 291 (1999) 413-418.
- 44- J. A. Noel, W. Teizer, W. H. Wang, *ACS Nano* 3 (2009) 1938–1946.

**E-4d****7d****E-4b**

Highlights

- New pyrrol-2(3*H*)-ones and pyridazin-3 (2*H*)-ones derivatives.
- Some compounds experienced good cytotoxic activity against HepG2 and MCF-7 cell lines.
- A pronounced inhibitory effect against cellular localization of tubulin.
- Molecular docking to colchicines binding site of tubulin using MOE program®.

ACCEPTED MANUSCRIPT